

## Citation:

Yasuda, T, Lewis, R and Adams, DJ 2004, 'Overexpressed Cavbeta3 inhibits N-type (Cav2.2) calcium channel currents through a hyperpolarizing shift of 'ultra-slow' and 'closed-state' inactivation', *Journal of General Physiology*, vol. 123, no. 4, pp. 401-416.

# Overexpressed $\text{Ca}_v\beta 3$ Inhibits N-type ( $\text{Ca}_v 2.2$ ) Calcium Channel Currents through a Hyperpolarizing Shift of "Ultra-slow" and "Closed-state" Inactivation

TAKAHIRO YASUDA,<sup>1</sup> RICHARD J. LEWIS,<sup>1,2</sup> AND DAVID J. ADAMS<sup>1</sup>

<sup>1</sup>School of Biomedical Sciences and <sup>2</sup>Institute for Molecular Bioscience, The University of Queensland, Queensland 4072, Australia

**ABSTRACT** It has been shown that  $\beta$  auxiliary subunits increase current amplitude in voltage-dependent calcium channels. In this study, however, we found a novel inhibitory effect of  $\beta 3$  subunit on macroscopic  $\text{Ba}^{2+}$  currents through recombinant N- and R-type calcium channels expressed in *Xenopus* oocytes. Overexpressed  $\beta 3$  (12.5 ng/cell cRNA) significantly suppressed N- and R-type, but not L-type, calcium channel currents at "physiological" holding potentials (HPs) of  $-60$  and  $-80$  mV. At a HP of  $-80$  mV, coinjection of various concentrations (0–12.5 ng) of the  $\beta 3$  with  $\text{Ca}_v 2.2\alpha_1$  and  $\alpha_2\delta$  enhanced the maximum conductance of expressed channels at lower  $\beta 3$  concentrations but at higher concentrations ( $>2.5$  ng/cell) caused a marked inhibition. The  $\beta 3$ -induced current suppression was reversed at a HP of  $-120$  mV, suggesting that the inhibition was voltage dependent. A high concentration of  $\text{Ba}^{2+}$  (40 mM) as a charge carrier also largely diminished the effect of  $\beta 3$  at  $-80$  mV. Therefore, experimental conditions (HP, divalent cation concentration, and  $\beta 3$  subunit concentration) approaching normal physiological conditions were critical to elucidate the full extent of this novel  $\beta 3$  effect. Steady-state inactivation curves revealed that N-type channels exhibited "closed-state" inactivation without  $\beta 3$ , and that  $\beta 3$  caused an  $\sim 40$ -mV negative shift of the inactivation, producing a second component with an inactivation midpoint of approximately  $-85$  mV. The inactivation of N-type channels in the presence of a high concentration (12.5 ng/cell) of  $\beta 3$  developed slowly and the time-dependent inactivation curve was best fit by the sum of two exponential functions with time constants of 14 s and 8.8 min at  $-80$  mV. Similar "ultra-slow" inactivation was observed for N-type channels without  $\beta 3$ . Thus,  $\beta 3$  can have a profound negative regulatory effect on N-type (and also R-type) calcium channels by causing a hyperpolarizing shift of the inactivation without affecting "ultra-slow" and "closed-state" inactivation properties.

**KEY WORDS:** voltage-dependent calcium channel • *Xenopus* oocyte •  $\beta 3$  auxiliary subunit • negative regulation • voltage-dependent inactivation

## INTRODUCTION

Voltage-dependent calcium channels (VDCCs) contribute to the electrical excitability of neurons and transduce electrical activity into other cellular functions, such as muscle contraction, pacemaker activity, neurotransmitter release, gene expression, or modulation of membrane excitability (for review see Berridge, 1997). High-voltage-activated calcium channels are comprised of a pore-forming  $\alpha_1$  subunit, auxiliary  $\beta$  and  $\alpha_2\delta$  subunits, and, in some cases, an auxiliary  $\gamma$  subunit (for review see Catterall, 2000). Based on  $\alpha_1$  gene similarity, they are divided into two families of L-type ( $\text{Ca}_v 1.1$ – $1.4$ ) and non-L-type calcium channels that include P/Q- ( $\text{Ca}_v 2.1$ ), N- ( $\text{Ca}_v 2.2$ ) and R-types ( $\text{Ca}_v 2.3$ ). Conserved transmembrane and pore domains of the  $\alpha_1$  subunits are  $\sim 50\%$  identical between the families and  $>80\%$  identical within a family (see Ertel et al., 2000). VDCC auxiliary  $\beta$

( $\text{Ca}_v\beta 1$ – $4$ ) and  $\alpha_2\delta$  ( $\text{Ca}_v\alpha_2\delta 1$ – $4$ ) subunits associate with the  $\alpha_1$  functional subunits (for review see Walker and De Waard, 1998) and affect the biophysical properties of the  $\alpha_1$  subunits as observed for the auxiliary subunits of voltage-dependent sodium and potassium channels (for review see Isom et al., 1994; Trimmer, 1998).

N-type calcium channels ( $\text{Ca}_v 2.2$ ) were pharmacologically characterized in chicken dorsal root ganglia neurons (Nowycky et al., 1985) and cloned together with their splice variants in mammalian central (Snutch et al., 1990; Dubel et al., 1992; Williams et al., 1992; Coppola et al., 1994; Lin et al., 1997; Kaneko et al., 2002) and peripheral neurons (Lin et al., 1997). Given that N-type channels, together with P/Q- and R-types, are distributed predominantly in presynaptic nerve terminals, they are involved in nerve-evoked release of neurotransmitter (for review see Waterman, 2000; Fisher and Bourque, 2001). Therefore, modulation of VDCC

Address correspondence to David J. Adams School of Biomedical Sciences, The University of Queensland, Queensland 4072, Australia. Fax: (07) 3365-4933; email: dadams@uq.edu.au

*Abbreviations used in this paper:* AID,  $\alpha_1$  subunit interaction domain; HP, holding potential; HVI, high-voltage inactivation; LVI, low-voltage inactivation; VDCC, voltage-dependent calcium channel.

currents by altering functional channel expression levels and biophysical properties is critical for regulation of neurotransmission in the nervous system. In particular, the amplitude and duration of macroscopic VDCC current, and hence intracellular  $\text{Ca}^{2+}$  concentration during action potentials, has significant effect on neurotransmitter release as the release is proportional to  $[\text{Ca}^{2+}]^m$ , where  $m$  takes a value from 2.5 to 4 (for review see Wu and Saggau, 1997).

With regard to the modulation of VDCC currents, both  $\beta$  and  $\alpha_2\delta$  subunits have been shown primarily to increase macroscopic current amplitude (Mori et al., 1991; Neely et al., 1993; Wakamori et al., 1993; Jones et al., 1998; Klugbauer et al., 1999). Coexpression of  $\beta$  subunits enhanced the level of channel expression in the plasma membrane (Williams et al., 1992; Brust et al., 1993) by chaperoning the translocation of  $\alpha_1$  subunits (Chien et al., 1995; Yamaguchi et al., 1998; Gao et al., 1999; Gerster et al., 1999) from ER where  $\beta$  subunits antagonize the binding between  $\alpha_1$  and an ER retention protein (Bichet et al., 2000). In addition,  $\beta$  subunits also increased channel open probability without affecting single-channel conductance (Neely et al., 1993; Wakamori et al., 1993, 1999; Jones et al., 1998; Gerster et al., 1999; Hohaus et al., 2000). A hyperpolarizing shift of I-V relationships by  $\beta$  subunits (Neely et al., 1993; Yamaguchi et al., 1998) also partially contributes to an increase in macroscopic current amplitude. The  $\beta$  subunit has been shown to interact with  $\alpha_1$  subunit interaction domain (AID) in the cytoplasmic I-II linker of  $\alpha_1$  subunit (Pragnell et al., 1994; Witcher et al., 1995), and all four  $\beta$  subunits interacted with AID of  $\text{Ca}_v2.2\alpha_1$  in vitro with high affinity ( $K_d$  of  $\sim 5$  nM; Scott et al., 1996). The interaction between  $\alpha_1$  and  $\beta$  subunits through AID plays a critical role in channel trafficking from the ER to plasma membrane (Gerster et al., 1999) and therefore VDCC current potentiation by  $\beta$  subunits (Pragnell et al., 1994; De Waard et al., 1995). On the other hand, coexpression of  $\alpha_2\delta$  subunits, like  $\beta$  subunits, augmented ligand binding ( $B_{\text{max}}$ ) and  $\alpha_1$  protein expression levels in the plasma membrane (Williams et al., 1992; Brust et al., 1993; Shistik et al., 1995) without increasing channel open probability and single-channel conductance (Bangalore et al., 1996; Jones et al., 1998; Wakamori et al., 1999) or shifting activation in a hyperpolarizing direction (Qin et al., 1998; Wakamori et al., 1999; Gao et al., 2000). The mechanism underlying  $\alpha_2\delta$ -induced potentiation of  $\alpha_1$  expression appears to be different from that of  $\beta$  subunits. A domain of  $\alpha_2\delta$ , which interacts with  $\alpha_1$  subunit, was proposed to be located in an extracellular region (Gurnett et al., 1997), and therefore it is unlikely that  $\alpha_2\delta$  subunits antagonize an interaction between an ER retention protein and an intracellular AID of  $\alpha_1$  subunits. Furthermore, lack of evidence for the  $\alpha_2\delta$ -induced  $\alpha_1$

subunit trafficking was shown using an immunohistochemical technique (Gao et al., 1999).

In contrast to VDCC current potentiation by auxiliary subunit, VDCCs are well known to be negatively regulated by G protein  $\beta\gamma$  subunits (for review see Zamponi, 2001) and this effect is modulated by calcium channel  $\beta$  subunits (Canti et al., 2000; Feng et al., 2001). Furthermore, syntaxin 1A, a key synaptic protein participating in neurotransmitter release, exerted an inhibitory effect on N- and Q-type calcium channels, thereby probably preventing  $\text{Ca}^{2+}$  overload or excessive neurotransmitter release (Bezprozvanny et al., 1995; Degtiar et al., 2000). Although VDCC auxiliary subunits positively regulate neurotransmitter release by enhancing neuronal (N-, P/Q- and R-type) calcium channel currents, there is less evidence for auxiliary subunit-induced negative regulation of these channels. Patil et al. (1998) have found pronounced channel inactivation during a train of action potential-like waveforms compared with a single square pulse for N-, P/Q- and R-type channels, and this was dependent on  $\beta$  subunit isoforms. In the present study, we characterize previously overlooked large negative regulatory effect of high levels of the  $\beta_3$  subunit on macroscopic currents carried by N- and R-type calcium channels. A preliminary report of these results, in part, has been presented in an abstract form (Yasuda et al., 2002).

## MATERIALS AND METHODS

### *Complimentary RNA Synthesis and Transient Expression in Oocytes*

Capped RNA transcripts encoding full-length VDCC pore-forming and auxiliary subunits, namely:  $\alpha_1$ , rat  $\text{Ca}_v2.2\alpha_1$  (former name  $\alpha_{1B}$ ) and rabbit  $\text{Ca}_v1.2\alpha_1$  ( $\alpha_{1C}$ );  $\beta$ , rat  $\beta_3$  and *Xenopus*  $\beta_3\text{xo}$ ; and  $\alpha_2\delta$ , rabbit  $\alpha_2\delta_1$ , were synthesized using the mMessage mMachine in vitro transcription kit (Ambion). Stage V-VI oocytes were removed from anesthetized female *Xenopus laevis* and treated for 2-3 h with 2.5 mg/ml collagenase (Type I; Sigma-Aldrich) for defolliculation. The oocytes were then injected with either an  $\alpha_1$  subunit alone, or in combination with an  $\alpha_2\delta$  and/or a  $\beta$  subunit. Except for rat  $\text{Ca}_v2.3\alpha_1$  ( $\alpha_{1E}$ ), of which cDNA was injected intranuclearly at a volume of 9.4 nl, 50 nl of cRNA mixtures were injected into the oocytes using an automatic microinjector (Drummond). The injected cells were incubated at 18°C in a ND96 solution (in mM): 96 NaCl, 2 KCl, 1  $\text{CaCl}_2$ , 1  $\text{MgCl}_2$ , 5 HEPES, 5 pyruvic acid, and 50  $\mu\text{g}/\text{ml}$  gentamicin, pH 7.5, before recording.

### *Electrophysiological Recordings*

3-8 d after the cRNA/cDNA injection, whole-cell calcium channel currents were recorded from the oocytes using the two-electrode voltage-clamp technique with Axon GeneClamp500B (Axon Instruments, Inc.). Voltage-recording and current-passing microelectrodes were filled with 3 M KCl and typically had resistances of 0.5-1.5 M $\Omega$  and 0.3-0.7 M $\Omega$ , respectively. Ionic currents were often of the order of several microamperes in amplitude, which resulted in a significant voltage error due to a voltage drop across resistance of a ground electrode. To minimize this error,

an independent two-electrode virtual-ground circuit with a 3 M KCl agar bridge was used. Unless stated otherwise, all recordings were made with a bath solution containing 5 mM  $\text{Ba}^{2+}$  as a charge carrier of which composition was (in mM): 5  $\text{BaCl}_2$ , 85 tetraethylammonium hydroxide (TEAOH), 5 KCl, 5 HEPES, titrated to pH 7.4 with methanesulfonic acid. When 5 mM  $\text{CaCl}_2$  was substituted for 5 mM  $\text{BaCl}_2$ , other components of the bath solution remained the same. When 40 mM  $\text{BaCl}_2$  was used, TEAOH was reduced to 42.5 mM. Oocytes were perfused continuously at a rate of  $\sim 1.5$  ml/min at room temperature ( $\sim 22^\circ\text{C}$ ). Activation of  $\text{Cl}^-$  currents was eliminated by injecting 25–50 nl of 50 mM 1,2-bis(o-aminophenoxy)ethane- $\text{N,N,N',N'}$ -tetraacetate (BAPTA) at least 15 min before recording. Most oocytes exhibited considerable run-down or run-up at the beginning of recording and experiment did not commence until fluctuation of peak currents with repeated depolarizing pulses reduced to less than  $\pm 2\%$  within a 1-min period. During the study of inactivation kinetics, if oocytes exhibited  $>120\%$  recovery from inactivation, experiments were repeated using the same oocytes.

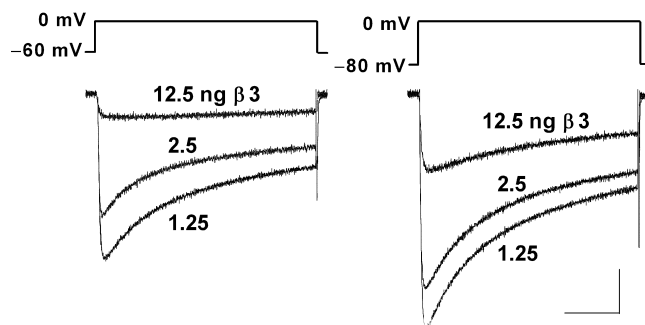
Using pCLAMP 8 software (Axon Instruments, Inc.), membrane currents were acquired at 10 kHz after a low-pass filter at 1 kHz and an on-line leak-subtraction with a -P/4 pulse protocol. I-V relationships were obtained by step depolarization from  $-80$

to  $+50$  mV in 10-mV increments, from holding potentials (HPs) of either  $-80$  or  $-120$  mV, with a 4-min interval between I-V curves obtained at each HP. For steady-state inactivation, unless stated otherwise, the HP was changed from  $-120$  to 0 mV in 5- or 10-mV increments, with each HP maintained for 3 min before each test pulse. Steady-state inactivation curves were derived from peak currents elicited by a test pulse to 0 mV given at the end of each HP. Normalized currents were calculated by dividing each peak current by that observed at a HP of  $-120$  mV.

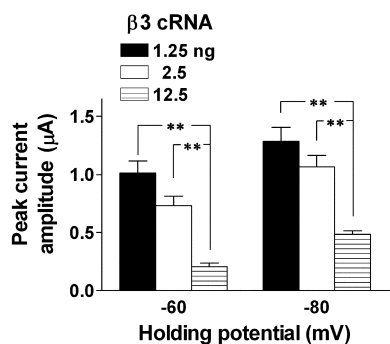
#### Data Analysis

Data were analyzed using Prism 3.0 (GraphPad). Each I-V relationship was fitted with smooth curves derived from a Boltzmann equation:  $I = G_{\text{max}}(V_t - E_{\text{rev}})/\{1 + \exp[(V_{1/2, \text{act}} - V_t)/k_{\text{act}}]\}$ , where  $G_{\text{max}}$  is the maximum conductance,  $V_t$  is the test potential,  $E_{\text{rev}}$  is the apparent reversal potential,  $V_{1/2, \text{act}}$  is the midpoint of activation, and  $k_{\text{act}}$  is the slope factor. Ratios of  $G_{\text{max}}$  ( $G_{\text{max}}$  at a HP of  $-120$  mV/ $G_{\text{max}}$  at a HP of  $-80$  mV) were calculated as an index of voltage-dependent inhibition. For steady-state inactivation, each data was fitted by a single Boltzmann equation:  $I/I_{-120} = 1/[1 + \exp((V_{1/2, \text{inact}} - V_t)/k_{\text{inact}})]$ , where  $V_{1/2, \text{inact}}$  is the midpoint of inactivation,  $k_{\text{inact}}$  is the slope factor, and  $I_{-120}$  is

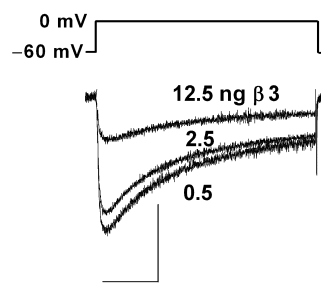
#### A $\text{Ca}_v2.2\alpha_1/\beta_3/\alpha_2\delta_1$



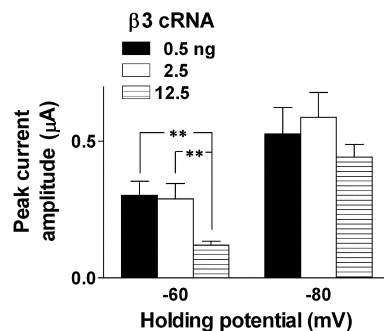
#### B $\text{Ca}_v2.2\alpha_1/\beta_3/\alpha_2\delta_1$



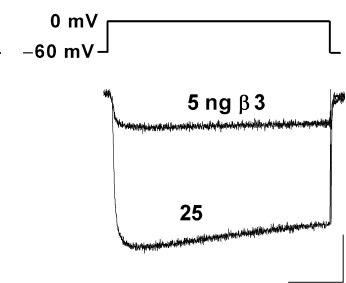
#### C $\text{Ca}_v2.3\alpha_1/\beta_3/\alpha_2\delta_1$



#### D $\text{Ca}_v2.3\alpha_1/\beta_3/\alpha_2\delta_1$



#### E $\text{Ca}_v1.2\alpha_1/\beta_3/\alpha_2\delta_1$



#### F $\text{Ca}_v1.2\alpha_1/\beta_3/\alpha_2\delta_1$

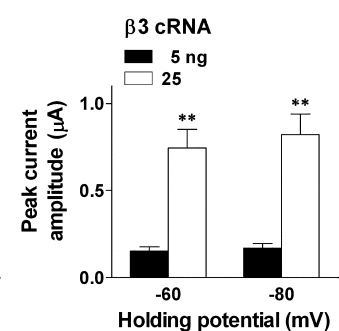


FIGURE 1. The  $\beta_3$  subunit markedly suppressed the current amplitude of N-type ( $\text{Ca}_v2.2$ ; A and B) and R-type ( $\text{Ca}_v2.3$ ; C and D), but not L-type ( $\text{Ca}_v1.2$ ; E and F) calcium channels at physiological HPs in *Xenopus* oocytes. For N- and R-type channels, cells were injected with cRNAs (cDNA for  $\text{Ca}_v2.3\alpha_1$  encoding either  $\text{Ca}_v2.2\alpha_1$  (2.5 ng/cell) or  $\text{Ca}_v2.3\alpha_1$  (4.5 ng/cell) and  $\alpha_2\delta_1$  (2.5 ng/cell) in combination with  $\beta_3$  (1.25, 2.5, or 12.5 ng/cell). Cells expressed L-type channels were injected with cRNA encoding  $\text{Ca}_v1.2\alpha_1$  (5 ng/cell) and  $\alpha_2\delta_1$  (12.5 ng/cell) in combination with  $\beta_3$  (5 or 25 ng/cell). Currents were evoked by a brief depolarization to 0 mV from HPs of  $-60$  and  $-80$  mV. (A, C, and E) Superimposed current traces of whole cell  $\text{Ba}^{2+}$  currents through the calcium channels. Bars, 0.5  $\mu\text{A}$  and 50 ms. Residual capacitance transients after leak subtraction have been erased. (B, D, and F) Summary of the effects of the  $\beta_3$  subunit on the peak currents of N- ( $n = 9$ ), R- ( $n = 7$ ), and L-type ( $n = 4$ ) calcium channels. Data are indicated as mean  $\pm$  SE. Asterisks denote significant difference between any two groups in each set of experiments (\*\* $P < 0.01$ ; one-way ANOVA with Bonferroni's multiple comparison test for B and D and unpaired  $t$ -test for F).

the control current amplitude at HP of  $-120$  mV, or a dual Boltzmann equation:  $I/I_{-120} = I_{LVI}\{1/[1 + \exp((V_{1/2, \text{inact LVI}} - V_i)/k_{LVI})]\} + I_{HVI}\{1/[1 + \exp((V_{1/2, \text{inact HVI}} - V_i)/k_{HVI})]\}$ , where LVI and HVI are low- and high-voltage inactivation, respectively, and  $I_{LVI}$  and  $I_{HVI}$  are the normalized current amplitudes ( $I_{LVI} + I_{HVI} = 1$ ). Unless stated otherwise, the goodness-of-fit of both equations was compared with  $F$ -test to achieve best fit.

#### Complimentary DNA Clones of $\text{Ca}^{2+}$ Channel Subunits

The  $\text{Ca}_v2.2\alpha_1$  (the central nerve splice variant  $\alpha_{1B-d}$ ) and  $\beta_3$  cDNAs were provided by Dr. D. Lipscombe (Brown University, Providence, RI);  $\text{Ca}_v1.2\alpha_1$  and  $\text{Ca}_v2.3\alpha_1$  cDNAs were provided by Dr. G. Zamponi (University of Calgary, Calgary, AL);  $\alpha_2\delta_1$  cDNA was provided by Dr. F. Hofmann and Dr. N. Klugbauer (Technische Universität München, Germany); and *Xenopus*  $\beta_3\text{xo}$  cDNA was provided by Dr. L. Birnbaumer (UCLA, Los Angeles, CA).

### $\text{Ca}_v2.2\alpha_1/\beta_3/\alpha_2\delta_1$

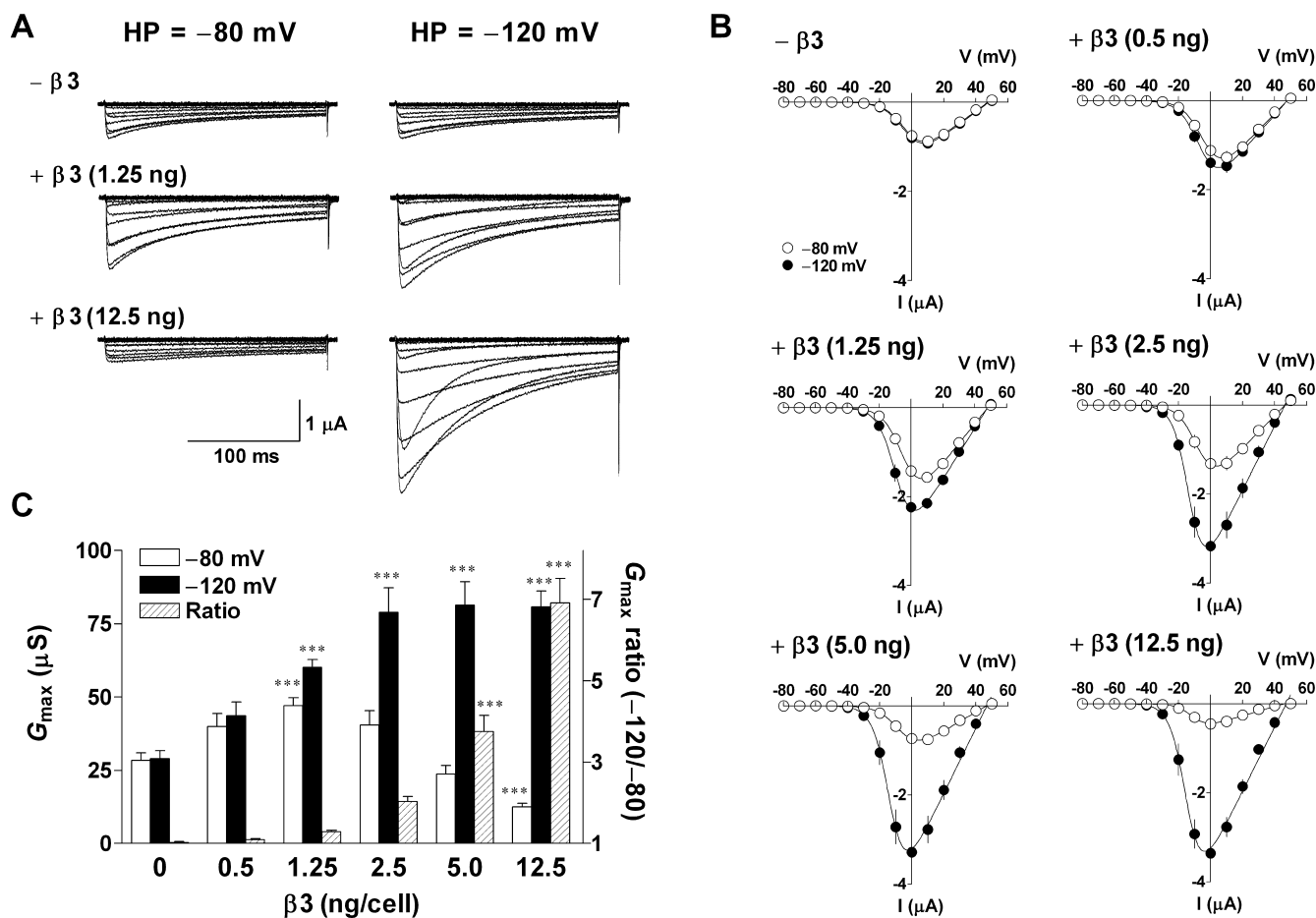


**FIGURE 2.** The  $\beta_3$  subunit caused a biphasic effect on N-type calcium channels at a physiological HP. Oocytes were injected with cRNAs encoding  $\text{Ca}_v2.2\alpha_1$  (2.5 ng/cell) and  $\alpha_2\delta_1$  (2.5 ng/cell) in combination with various concentrations of  $\beta_3$  (0, 0.5, 1.25, 2.5, 5, or 12.5 ng/cell). (A) Examples of whole cell  $\text{Ba}^{2+}$  currents at HPs of  $-80$  mV (left) and  $-120$  mV (right). (B) Corresponding I-V relationships for peak  $\text{Ba}^{2+}$  currents at HPs of  $-80$  (open circle) and  $-120$  mV (closed circle). Activation midpoints ( $V_{1/2, \text{act}}$  at the HPs of  $-80$  and  $-120$  mV) calculated from the Boltzmann fitting are:  $\beta_3$  0 ng,  $-2.7$  and  $-3.0$  mV; 0.5 ng,  $-3.4$  and  $-5.8$  mV; 1.25 ng,  $-4.1$  and  $-8.5$  mV; 2.5 ng,  $-5.9$  and  $-12.4$  mV; 5.0 ng,  $-6.8$  and  $-13.3$  mV; 12.5 ng,  $-10.7$  and  $-14.7$  mV, respectively. (C) Effects of the  $\beta_3$  subunit on the maximum conductance ( $G_{\max}$ ) at the HPs of  $-80$  (open column) and  $-120$  mV (closed column) and the  $G_{\max}$  ratio (hatched column). Data are indicated as mean  $\pm$  SE ( $n = 11$ – $12$  from two frogs). Asterisks denote significant difference versus the control group without  $\beta_3$  (\*\*\*) ( $P < 0.001$ ; one-way ANOVA with Dunnett's multiple comparison test).

## RESULTS

### Suppression of N- ( $\text{Ca}_v2.2$ ) and R-type ( $\text{Ca}_v2.3$ ) Calcium Channel Currents by $\beta_3$ Subunit

*Xenopus* oocytes coinjected with 2.5 ng/cell of  $\text{Ca}_v2.2\alpha_1$  and  $\alpha_2\delta$  and 1.25 ng/cell of  $\beta_3$ , produced robust  $\text{Ba}^{2+}$  currents through open N-type calcium channels in response to a step depolarization to 0 mV from HPs of  $-60$  and  $-80$  mV (Fig. 1 A). The peak current amplitude was significantly reduced and inactivation kinetics slowed in a concentration-dependent manner by increasing concentrations of  $\beta_3$  (Fig. 1, A and B). The effect was more pronounced at the more positive HP of



–60 mV, where an 80% reduction in peak current amplitude was observed with injection of 12.5 ng  $\beta 3$ . Although a similar  $\beta 3$ -induced inhibitory effect was observed on R-type ( $\text{Ca}_v2.3$ ) calcium channels, it was less pronounced than for N-type channels (Fig. 1, C and D). In contrast, injection of 25 ng  $\beta 3$  subunit markedly enhanced L-type ( $\text{Ca}_v1.2$ ) calcium channel currents at both HPs (Fig. 1, E and F).

### $\beta 3$ Subunits Showed Biphasic Effects on N-type Calcium Channel Activation

Various concentrations of  $\beta 3$  subunit mRNA (0–12.5 ng/cell) were coinjected with  $\text{Ca}_v2.2\alpha_1$  and  $\alpha_2\delta$  subunits. As shown in Fig. 2, at a HP of –80 mV,  $\beta 3$  subunit exhibited a biphasic, bell-shaped effect on both peak amplitude of I-V curves and the maximum conductance ( $G_{\text{max}}$ ); that is, concentration-dependent enhancement at low concentrations (0–1.25 ng) and inhibition at high concentrations (2.5–12.5 ng).  $G_{\text{max}}$  was increased to a maximum by 1.25 ng  $\beta 3$  and was 1.7-fold higher than that of the control group in which N-type calcium channels were expressed without  $\beta 3$ . The peak  $G_{\text{max}}$  observed with 1.25 ng  $\beta 3$  was reduced by 74% in the presence of 12.5 ng  $\beta 3$ , which corresponds to 56% inhibition compared with the control group (Fig. 2 C).

To determine whether this inhibition by  $\beta 3$  may be attributed to voltage-dependent channel inactivation or other voltage-independent mechanisms such as inhibition of functional channel expression, the oocyte was held at –120 mV to remove voltage-dependent inactivation. At a HP of –120 mV,  $\beta 3$  enhanced the calcium channel current in a concentration-dependent manner, and the maximum current (2.8-fold enhancement compared with the control group) was obtained with 5 ng  $\beta 3$ . This result suggests that the inhibitory effect of  $\beta 3$  observed at –80 mV was due to voltage-dependent channel inactivation. The difference in concentration-dependence observed for  $G_{\text{max}}$  at –120 mV compared with that for  $G_{\text{max}}$  ratio suggests that two distinct mechanisms may underlie the effect of  $\beta 3$  subunit (Fig. 2 C).

### Effect of $\beta 3$ on Steady-state Inactivation

Since the  $\beta 3$ -induced current inhibition is voltage dependent, it was of interest to investigate the effects of the various concentrations of  $\beta 3$  on steady-state channel inactivation. To examine steady-state inactivation, oocytes were held at each HP for 3 min instead of brief conditioning pulses of 5–30 s. The  $\beta 3$  subunit produced a concentration-dependent leftward shift of the inactivation curve (Fig. 3 A). Significantly, the shift was

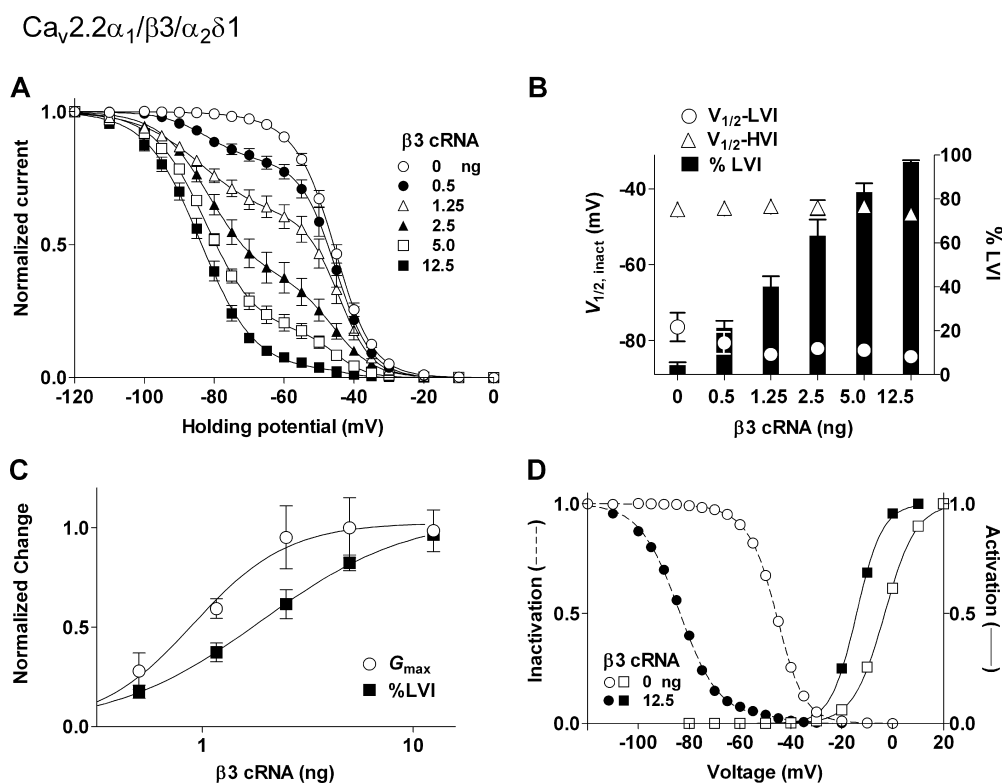


FIGURE 3. The  $\beta 3$ -induced hyperpolarizing shift of the steady-state inactivation curves of N-type calcium channels is attributed to change in the proportion of two components of the curves. Oocytes were injected with cRNAs as shown in Fig. 2. (A) Steady-state inactivation for HPs of 3-min duration. Data are indicated as mean  $\pm$  SE ( $n = 7$ –15 from 3–7 frogs for each group). Note that HPs of 3 min did not induce maximal inactivation and therefore reflect “pseudo-steady-state” inactivation (compare Fig. 8). (B) Effects of the  $\beta 3$  subunit on inactivation midpoints ( $V_{1/2, \text{inact}}$ ) of LVI (open circle) and HVI (open triangle) and the proportion of LVI (%LVI; closed column). Plotted data were derived from the curve fitting in panel A and shown as mean  $\pm$  SE. (C) Difference in concentration dependency of the  $\beta 3$ -induced enhancement of  $G_{\text{max}}$  and increase in the %LVI. Plotted data were derived from B and Fig. 2 C for %LVI and  $G_{\text{max}}$  at a HP of –120 mV, respectively. Data were normalized by dividing each value by the maximum value and are expressed as mean  $\pm$  SE. (D) No or little overlap of activation and inactivation curves seen in the presence or absence of  $\beta 3$ . Plotted data were derived from panel A and Fig. 2 B.

not a gradual parallel leftward shift of inactivation curves but instead the inactivation curve exhibited two components with different midpoints ( $V_{1/2, \text{inact}}$ ) of approximately  $-85$  and  $-45$  mV (Fig. 3 B). These components were termed low-voltage inactivation (LVI) and high-voltage inactivation (HVI), respectively. The  $V_{1/2, \text{inact}}$  of LVI and HVI were not significantly altered by  $\beta 3$  concentration, indicating that the  $\beta 3$ -induced hyperpolarizing shift of the inactivation curve was caused by either an increase in the proportion of the LVI (%LVI) or a decrease in %HVI (Fig. 3 B). This result is consistent with that reported previously for N-type calcium channels expressed in oocytes (Canti et al., 2001), where the existence of two components in inactivation with  $V_{1/2, \text{inact}}$  of approximately  $-70$  and  $-40$  mV was demonstrated with intranuclear injection of various concentrations of  $\beta 3$  cDNA. The more positive  $V_{1/2, \text{inact}}$  reported in their study may be due to a shorter prepulse of 25 s. The  $\beta 3$ -concentration dependence of  $G_{\text{max}}$  and %LVI were compared (Fig. 3 C). The  $EC_{50}$  value for %LVI (1.91 ng) was significantly different from that obtained for  $G_{\text{max}}$  (0.91 ng). The result likely explains the biphasic response of  $G_{\text{max}}$  at a HP of  $-80$  mV seen in Fig. 2 C. Subsequent kinetic experiments revealed that HPs of 3 min were of insufficient duration to induce maximal inactivation (see Fig. 8) and therefore more accurately reflect "pseudo-steady-state" inactivation.

*Xenopus* oocytes express an endogenous calcium channel  $\beta 3$  ( $\beta 3\text{xo}$ ) subunit, and the expression of calcium channel  $\alpha_1$  subunit alone ( $\text{Ca}_v1.2$ ,  $2.2$  or  $2.3\alpha_1$ ) in oocytes has been shown to be blocked by antisense injection for  $\beta 3\text{xo}$  (Tareilus et al., 1997; Canti et al., 2001). Therefore, it is possible that the  $\text{Ca}_v2.2\alpha_1$  subunit could interact with the endogenous  $\beta 3\text{xo}$ , especially when expressed without heterologous rat  $\beta 3$ . If this is the case, the two different  $V_{1/2, \text{inact}}$  observed could arise from different  $\beta 3$  subunits combining with the  $\alpha_1$  subunit such that HVI and LVI might originate from N-type calcium channels composed of  $\text{Ca}_v2.2\alpha_1/\beta 3\text{xo}/\alpha_2\delta$  and  $\text{Ca}_v2.2\alpha_1/\beta 3/\alpha_2\delta$ , respectively. This hypothesis was tested by coexpressing various concentrations of  $\beta 3\text{xo}$  with  $\text{Ca}_v2.2\alpha_1$  and  $\alpha_2\delta$ . Similar to the rat  $\beta 3$ , exogenous  $\beta 3\text{xo}$  not only enhanced the N-type channel current amplitude at the HP of  $-120$  mV (9.0-fold increase in  $G_{\text{max}}$ ), but also caused a leftward shift of the inactivation curve (Fig. 4). The maximum increase in  $G_{\text{max}}$  (9.0-fold) caused by  $\beta 3\text{xo}$  (Fig. 4 B) was much more pronounced than that (2.8-fold) by rat  $\beta 3$  (Fig. 2 C), although amino acid sequences for  $\beta 3$  exhibit a high similarity (Tareilus et al., 1997). Importantly, the  $\beta 3\text{xo}$ -induced leftward shift of inactivation is inconsistent with the idea that the rat  $\beta 3$ -induced leftward shift of the inactivation curve was dependent on the presence of  $\beta 3\text{xo}$ . Thus, the two components of inactivation curves may be due to two different forms of the N-type calcium channel caused by

### $\text{Ca}_v2.2\alpha_1/\beta 3\text{xo}/\alpha_2\delta 1$

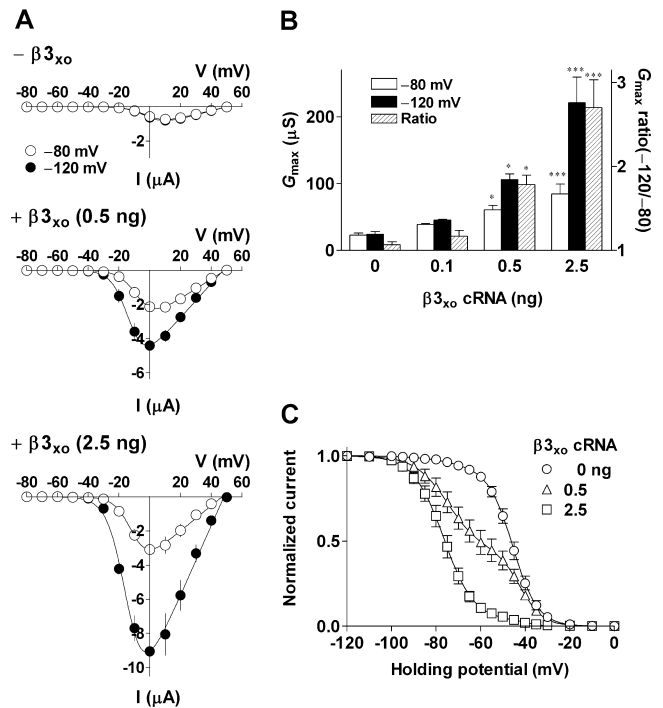


FIGURE 4. The oocyte  $\beta 3$  ( $\beta 3\text{xo}$ ) subunit injected exogenously with N-type calcium channels modified channel properties similar to that observed for the rat  $\beta 3$  subunit. Oocytes were injected with cRNAs encoding  $\text{Ca}_v2.2\alpha_1$  (2.5 ng/cell) and  $\alpha_2\delta$  (2.5 ng/cell) subunits in combination with various concentrations of  $\beta 3\text{xo}$  subunit (0, 0.1, 0.5, or 2.5 ng/cell). (A) I-V relationships for peak  $\text{Ba}^{2+}$  currents at HPs of  $-80$  mV (open circle) and  $-120$  mV (closed circle). (B) Effects of the  $\beta 3\text{xo}$  subunit on the maximum conductance ( $G_{\text{max}}$ ) at HPs of  $-80$  mV (open column) and  $-120$  mV (closed column) and  $G_{\text{max}}$  ratio (hatched column). (C) The  $\beta 3\text{xo}$  caused a leftward shift of the steady-state inactivation curve. Inactivation midpoints ( $V_{1/2, \text{inact}}$ ) were as follows:  $\beta 3\text{xo}$  0 ng (LVI and HVI),  $-72.6$  and  $-45.5$  mV; 0.5 ng,  $-74.7$  and  $-42.1$  mV; 2.5 ng,  $-75.4$  and  $-40.0$  mV. Proportions of LVI were as follows:  $\beta 3\text{xo}$  0 ng, 7.6%; 0.5 ng, 55.7%; 2.5 ng, 96.0%. Data are indicated as mean  $\pm$  SE (A and B,  $n = 5$  from 1 frog; C,  $n = 5-6$  from 2-3 frogs). Asterisks denote significant difference versus the control group without  $\beta 3$  (\* $P < 0.05$ , \*\*\* $P < 0.001$ ).

interactions with different levels of coexpressed  $\beta 3$  subunit. Although, at a HP of  $-80$  mV,  $\beta 3$  at higher concentrations inhibited  $G_{\text{max}}$ , resulting in a biphasic effect (Fig. 2 C);  $\beta 3\text{xo}$  simply enhanced channel  $G_{\text{max}}$  in a concentration-dependent manner (Fig. 4 B). This could be attributed to the difference in  $V_{1/2, \text{inact}}$  of LVI obtained with  $\beta 3$  and  $\beta 3\text{xo}$  which are approximately  $-85$  and  $-70$  mV, respectively.

There was minimal overlap between activation and inactivation curves with or without  $\beta 3$  as shown in Fig. 3 D, indicating that this voltage-dependent inactivation occurs during the "closed-state" of N-type channels. Although  $\beta 3$  caused hyperpolarizing shift of both activa-

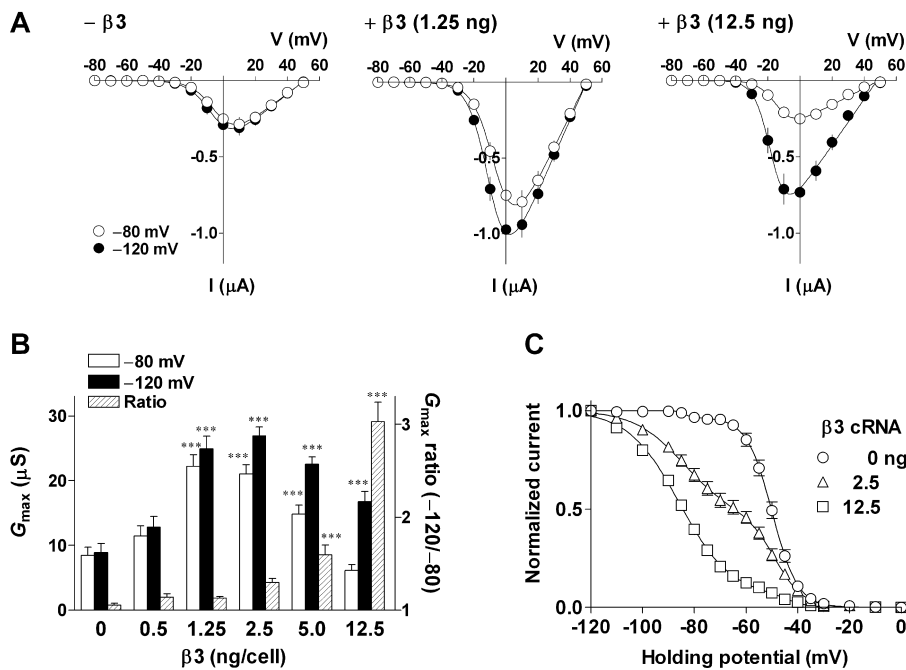
Ca<sub>v</sub>2.2α<sub>1</sub>/β3

FIGURE 5. The  $\alpha_2\delta$  subunit was not essential for the  $\beta_3$  subunit-induced inhibition of the N-type calcium channels. Oocytes were injected with cRNAs encoding Ca<sub>v</sub>2.2α<sub>1</sub> (2.5 ng/cell) in combination with various concentrations of  $\beta_3$ . (A) I-V relationships for the peak Ba<sup>2+</sup> currents at HPs of -80 (open circle) and -120 mV (closed circle). (B) Effects of the  $\beta_3$  subunit on the  $G_{\max}$  at different HPs.  $G_{\max}$  ratio (hatched column) was derived from  $G_{\max}$  at -80 (open column) and -120 mV (closed column). (C) Effect of the  $\beta_3$  subunit on steady-state inactivation. Inactivation midpoints ( $V_{1/2, \text{inact}}$ ) were calculated as follows:  $\beta_3$  0 ng (LVI and HVI), -66.7 and -49.8 mV; 2.5 ng, -84.2 and -48.6 mV; 12.5 ng, -85.7 and -44.3 mV. Proportions of LVI were as follows:  $\beta_3$  0 ng, 11.0%; 2.5 ng, 54.0%; 12.5 ng, 94.2%. Data are indicated as mean  $\pm$  SE (A and B,  $n = 11$  from 2 frogs; C,  $n = 4-8$  from 2-4 frogs). Asterisks denote significant difference versus the control group without  $\beta_3$  (\*\* $P < 0.01$ , \*\*\* $P < 0.001$ ).

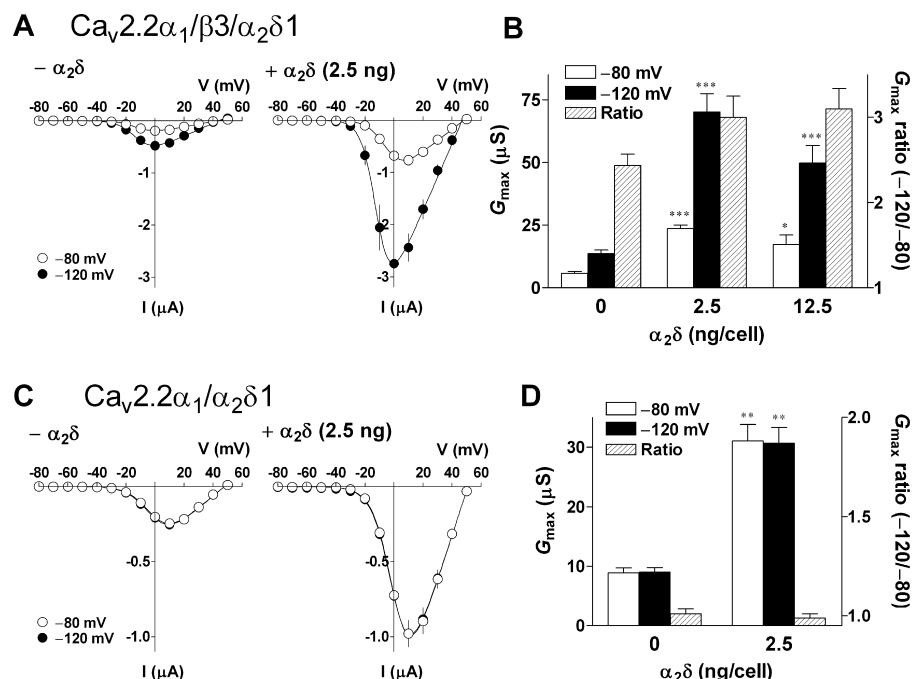
tion and inactivation curves, the effect on inactivation was more pronounced than on activation.

#### The $\alpha_2\delta$ Subunit Is Not Involved in the Down-regulation of N-type Calcium Channels

In the absence of  $\alpha_2\delta$ ,  $\beta_3$  caused a biphasic response and a hyperpolarizing shift of inactivation also observed in the presence of  $\alpha_2\delta$  (Fig. 5). This result indi-

cates that the  $\beta_3$  subunit does not require the  $\alpha_2\delta$  subunit for its effects. Higher concentrations of  $\beta_3$  (5 and 12.5 ng) inhibited  $G_{\max}$  even at a holding potential of -120 mV (Fig. 5 B). The underlying mechanism of this additional channel inhibition is unknown. To determine whether the inactivation is voltage dependent, further investigation with more negative HPs may be warranted, but it is unlikely to be attributed to competi-

FIGURE 6. The  $\alpha_2\delta$  subunit markedly enhanced  $G_{\max}$  of the N-type calcium channels but had little or no effect on  $G_{\max}$  ratio. Oocytes were injected with cRNAs encoding Ca<sub>v</sub>2.2α<sub>1</sub> (2.5 ng/cell) in combination with  $\alpha_2\delta$  (0, 2.5, or 12.5 ng/cell) in the presence (A and B) or absence (C and D) of the  $\beta_3$  subunit (2.5 ng/cell). (A and C) I-V relationships for the peak Ba<sup>2+</sup> currents at HPs of -80 mV (open circle) and -120 mV (closed circle). (B and D) Effects of the  $\alpha_2\delta$  subunit on  $G_{\max}$  at HPs of -80 (open column) and -120 mV (closed column) and  $G_{\max}$  ratio (hatched column). Data are indicated as mean  $\pm$  SE (A and B,  $n = 5-6$ ; C and D,  $n = 6$  from 1 frog each). Asterisks denote significant difference versus the control group without  $\beta_3$  (\* $P < 0.05$ , \*\* $P < 0.01$ , \*\*\* $P < 0.001$ ).



tion of RNA translation or toxicity produced by high levels of RNA because the same concentration of  $\beta 3$  did not exhibit this effect in the presence of  $\alpha_2\delta$  (Fig. 3).

Like the  $\beta$  subunits,  $\alpha_2\delta$  is also known to enhance VDCC currents (Klugbauer et al., 1999). To confirm whether  $\alpha_2\delta$  exhibits a biphasic effect on the calcium channel current due to a voltage-dependent inactivation, the effects of  $\alpha_2\delta$  on  $G_{\max}$  and  $G_{\max}$  ratio were examined. In the presence of  $\beta 3$  (2.5 ng),  $\alpha_2\delta$  enhanced the current by 4.1-fold at  $-80$  mV, but had no significant effect on the  $G_{\max}$  ratio (Fig. 6, A and B). A similar result was obtained in the absence of  $\beta 3$ , where  $\alpha_2\delta$  enhanced currents by 3.5-fold at  $-80$  mV but did not change the  $G_{\max}$  ratio (Fig. 6, C and D). In contrast to the  $\beta 3$  subunit, the  $\alpha_2\delta$  subunit enhanced N-type calcium channel current amplitude without a significant negative regulatory effect.

#### Effects of $\beta 3$ Subunit on R- and L-type Calcium Channels

Analogous to the effect on N-type calcium channels,  $\beta 3$  exhibited a biphasic response in  $G_{\max}$  (Fig. 7, A and B) of R-type calcium channels at a HP of  $-80$  mV. In comparison with a control group without the  $\beta 3$  subunit,  $\beta 3$  at 0.5 and 2.5 ng increased  $G_{\max}$  slightly and decreased it at a higher concentration of 12.5 ng, which is in agreement with the data shown in Fig. 1, C and D. At a HP of  $-120$  mV,  $\beta 3$  enhanced  $G_{\max}$  in a concentration-dependent manner although the enhancement (1.8-fold compared with control) was less pronounced than that observed for N-type channels (2.8-fold). Concomitant with increase in the  $G_{\max}$  ratio (Fig. 7 B), the inactivation of R-type channels was shifted negatively by  $\beta 3$  with  $V_{1/2, \text{inact}}$  for LVI and HVI of approximately  $-85$  and  $-60$  mV, respectively (Fig. 7 C). In contrast,  $\beta 3$  caused only an increase in  $G_{\max}$  of L-type channels at both HPs of  $-80$  and  $-120$  mV without any suppression of  $G_{\max}$  or a significant change in  $G_{\max}$  ratio (Fig. 7, D and E). Furthermore,  $\beta 3$  did not cause a leftward shift of inactivation but rather a slight rightward shift (Fig. 7 F). Thus, the biphasic effect of  $\beta 3$  is not general feature of all types of high-voltage activated calcium channels.

#### Kinetics of the Closed-state Inactivation of N- and R-type Calcium Channels

The closed-state inactivation kinetics of N- and R-type calcium channels was examined in the presence and absence of  $\beta 3$  subunit. Closed-state inactivation was induced by altering the HP, as indicated in Fig. 8, A–D, and channel activity was assessed using brief depolarizations at 20-s intervals from each HP. For inactivation kinetics, the HP was shifted from a voltage at which channels were not inactivated to that of approximately  $V_{1/2, \text{inact}}$  without eliciting channel activation (see Figs. 3 A

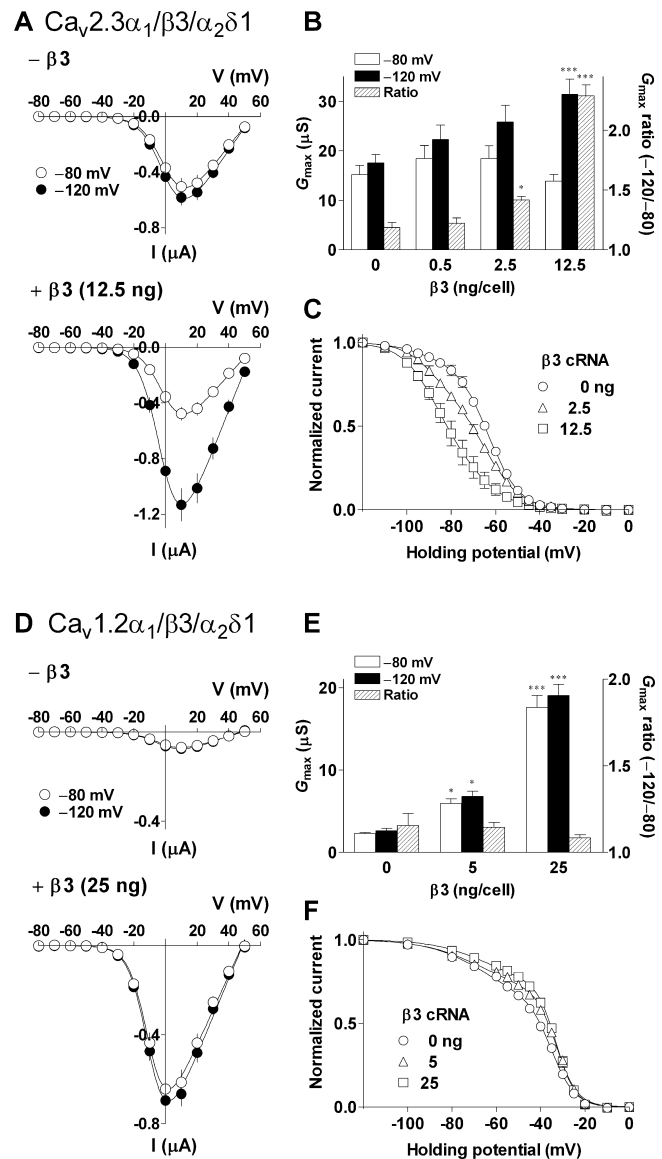
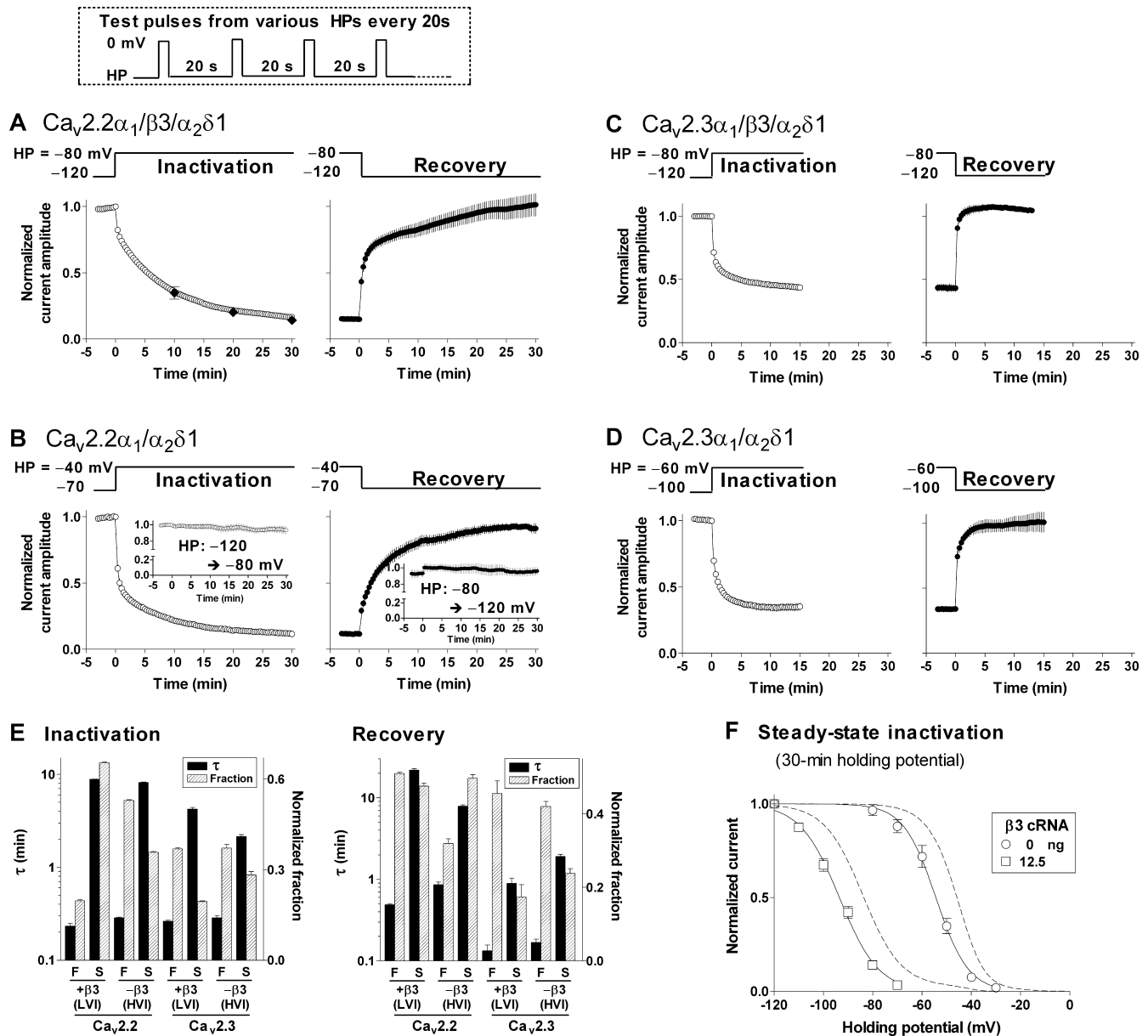


FIGURE 7. Effects of the  $\beta 3$  subunit on R- (A–C) and L- (D–F) type calcium channels. For R-type channels, oocytes were injected with cRNA (cDNA for  $\alpha_1$ ) encoding  $\text{Ca}_v2.3\alpha_1$  (4.5 ng/cell) and  $\alpha_2\delta$  (2.5 ng/cell) in combination with various concentrations of  $\beta 3$  (0, 0.5, 2.5 or 12.5 ng/cell). Cells expressing L-type channels were injected with cRNA encoding  $\text{Ca}_v1.2\alpha_1$  (5 ng/cell),  $\alpha_2\delta$  (12.5 ng/cell), and  $\beta 3$  (0, 5, or 25 ng/cell). (A and D) I–V relationships for the peak  $\text{Ba}^{2+}$  currents at HPs of  $-80$  mV (open circle) and  $-120$  mV (closed circle). (B and E) Effects of the  $\beta 3$  subunit on  $G_{\max}$  at different HPs.  $G_{\max}$  ratio (hatched column) was calculated from  $G_{\max}$  at  $-80$  (open column) and  $-120$  mV (closed column). (C and F) Effect of the  $\beta 3$  subunit on steady-state inactivation. Inactivation midpoints ( $V_{1/2, \text{inact}}$ ) were as follows: R-type/ $\beta 3$  0 ng (LVI and HVI),  $-94.7$  and  $-63.3$  mV; 2.5 ng,  $-89.5$  and  $-64.7$  mV; 12.5 ng,  $-86.5$  and  $-58.5$  mV; L-type/ $\beta 3$  0 ng (LVI and HVI),  $-65.3$  and  $-35.0$  mV; 5 ng,  $-67.1$  and  $-32.8$  mV; 25 ng,  $-64.2$  and  $-33.0$  mV. Proportion of LVI was as follows: R-type/ $\beta 3$  0 ng, 10.6%; 2.5 ng, 28.3%; 12.5 ng, 90.8%; L-type/ $\beta 3$  0 ng, 38.8%; 5 ng, 31.9%; 25 ng, 28.7%. Data are indicated as mean  $\pm$  SE (A and B,  $n = 8$  from 2 frogs; C,  $n = 4$ –7 from 2 frogs; D and E,  $n = 5$  from 1 frog; F,  $n = 4$  from 1 frog). Asterisks denote significant difference versus the control group without  $\beta 3$  (\* $P < 0.05$ , \*\*\* $P < 0.001$ ).





**FIGURE 8.** Slow kinetics of the closed-state inactivation of N- and R-type calcium channels. Oocytes were injected with cRNAs (cDNA for  $Ca_v2.3\alpha_1$ ) encoding either  $Ca_v2.2\alpha_1$  (2.5 ng/cell) or  $Ca_v2.3\alpha_1$  (4.5 ng/cell) and  $\alpha_2\delta$  (2.5 ng/cell) in the absence or presence of  $\beta3$  (12.5 ng/cell). The kinetics of the inactivation and the recovery from the inactivation were investigated by altering HPs as indicated in each panel (A–D). Kinetic curves were derived from peak currents elicited by repetitive test pulses (100 ms) to 0 mV every 20 s as shown in the top. (A and B) Inactivation kinetics of N-type calcium channels.  $Ca_v2.2\alpha_1$  with (A) or without  $\beta3$  (B) corresponds to LVI or HVI of the steady-state inactivation curve of N-type channels, respectively (see Fig. 3 A). Closed diamonds in A are inactivation kinetics when channel activity was tested every 10 min instead of at 20-s intervals ( $n = 4$ ). Inserts in B are control experiments indicating stable channel activity during a whole experiment ( $n = 8$ ). (C and D) Inactivation kinetics of R-type calcium channels.  $Ca_v2.3\alpha_1$  with (C) or without  $\beta3$  (D) corresponds to LVI or HVI of the steady-state inactivation curve of R-type channels, respectively (see Fig. 7 C). All the inactivation and recovery kinetic curves were fitted statistically better to a two-phase exponential than to a mono exponential function ( $F$ -test). (E) Time constants ( $\tau$ ) and corresponding fractions for the kinetics of inactivation and recovery from the inactivation. F and S indicate a fast and a slow component, respectively. Data are indicated as mean  $\pm$  SE ( $n = 4$ –6 from 2 frogs). (F) Steady-state inactivation with 30-min HPs. Broken lines show inactivation curves obtained with 3-min HPs for comparison (see Fig. 3 A). Each data point was obtained from individual oocytes and represents mean  $\pm$  SE ( $n = 4$ –5 from 2–3 frogs).

and 7 C). For example, oocytes expressing N-type channels with 12.5 ng  $\beta3$  were held at  $-120$  mV for 3 min and then the HP was changed to  $-80$  mV to induce

channel inactivation (Fig. 8 A). The closed-state inactivation in the presence of a high concentration (12.5 ng) of  $\beta3$  developed slowly and the time-dependent in-

activation curve was best fit by the sum of two exponential functions with time constants ( $\tau$ ) of 14 s and 8.8 min (Fig. 8, A and E). Test pulses with longer intervals of 10 min did not alter the kinetics (Fig. 8 A, closed diamonds), suggesting there is no accumulated inactivation caused by repetitive depolarization. The recovery from the inactivation was similarly very slow with time constants of 29 s and 21.8 min (Fig. 8, A and E). Similar slow kinetics for the onset and recovery from inactivation were observed for N-type channels expressed without  $\beta 3$  (Fig. 8, B and E). N-type channels expressed with or without the high concentration (12.5 ng) of  $\beta 3$  mainly exhibit LVI or HVI, respectively (see Fig. 3 B), and therefore the very slow closed-state inactivation observed independent of  $\beta 3$  is a common property of two different states or compositions (LVI and HVI) of N-type channels. Thus, each inactivation component, LVI or HVI, has been shown to represent the net effect of a kinetically complex inactivation process with at least two exponential components. In other words,  $\beta 3$  simply shifts the voltage dependence of the closed-state inactivation in a hyperpolarizing direction and does not substantially affect the inactivation kinetics. Similar results were obtained for R-type calcium channels (Fig. 8, C–E). Although inactivation kinetics of R-type channels were faster than for N-type channels, the time constant of the slow component was still in the order of minutes.

Considering the extremely slow kinetics of N-type channels, the steady-state inactivation was reexamined with longer duration HPs of 30 min. As predicted from the kinetics results, the longer HPs caused a significant negative shift of inactivation curves, and the  $V_{1/2, \text{inact}}$  for HVI without  $\beta 3$  or LVI with 12.5 ng  $\beta 3$  calculated using single Boltzmann fitting were  $-54.4$  or  $-93.5$  mV, respectively (Fig. 8 F).

#### Effect of Divalent Cations on Voltage-dependent Inactivation of N-type Calcium Channels

It is well known that different species and concentration of divalent cations can affect the voltage dependence of ion channel gating (for review see Hille, 2001). To determine whether the  $\beta 3$ -induced current suppression is observed with the physiological divalent ion,  $\text{Ca}^{2+}$ , the biophysical properties of N-type channels expressed in the absence and presence of  $\beta 3$  (12.5 ng/cell) were examined with 5 mM  $\text{Ca}^{2+}$  as a charge carrier. Although  $G_{\text{max}}$  was reduced by half with 5 mM  $\text{Ca}^{2+}$  compared with that obtained with 5 mM  $\text{Ba}^{2+}$  in the presence of  $\beta 3$ , the  $G_{\text{max}}$  ratio of 5.1 obtained with 5 mM  $\text{Ca}^{2+}$  was close to that of 6.4 obtained with 5 mM  $\text{Ba}^{2+}$  (Fig. 9, A and B). The comparable  $G_{\text{max}}$  ratios were attributed to similar  $V_{1/2, \text{inact}}$  of  $-81.0$  and  $-85.4$  mV with 5 mM  $\text{Ca}^{2+}$  and 5 mM  $\text{Ba}^{2+}$ , respectively (Fig. 9 C). The  $\beta 3$ -induced negative shifts in inactivation under both conditions were also comparable as the differ-

### $\text{Ca}_v2.2\alpha_1/\beta 3/\alpha_2\delta 1$

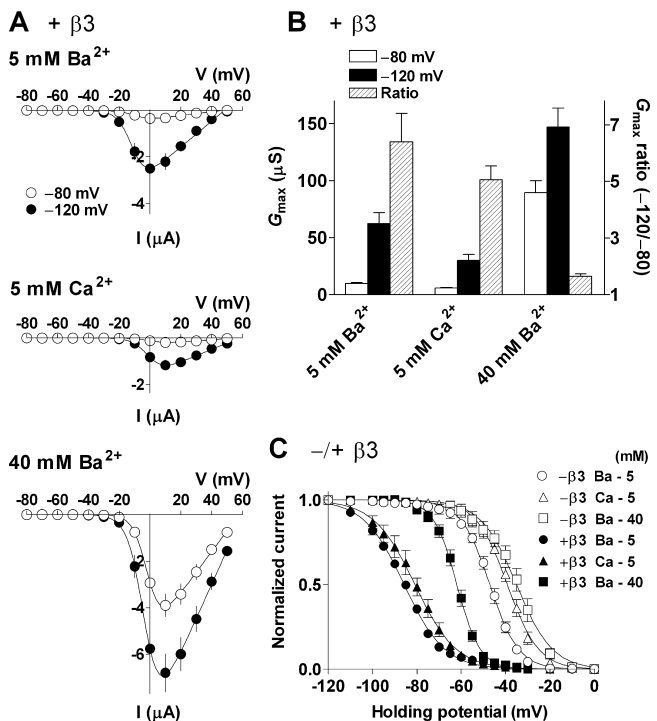


FIGURE 9. Effects of different charge carriers (divalent cations) on the  $\beta 3$  subunit-induced inactivation of N-type calcium channels. Oocytes were injected with cRNAs encoding  $\text{Ca}_v2.2\alpha_1$  (2.5 ng/cell),  $\alpha_2\delta$  (2.5 ng/cell) and  $\beta 3$  (12.5 ng/cell). Recording was performed with a bath solution containing 5 or 40 mM  $\text{Ba}^{2+}$ , or 5 mM  $\text{Ca}^{2+}$  as the charge carrier. (A) I-V relationships for the peak divalent cation currents at HPs of  $-80$  (open circle) and  $-120$  mV (closed circle). (B) Effects of the different charge carriers on  $G_{\text{max}}$  at HPs of  $-80$  (open column) and  $-120$  mV (closed column) and  $G_{\text{max}}$  ratio (hatched column). (C) Effects of the different charge carriers on steady-state inactivation. For simple comparison, inactivation midpoints ( $V_{1/2, \text{inact}}$ ) obtained with and without  $\beta 3$  were derived from a single Boltzmann equation: 5 mM  $\text{Ba}^{2+}$  ( $-\beta 3$  and  $+\beta 3$ ),  $-47.3$  and  $-85.4$  mV; 5 mM  $\text{Ca}^{2+}$ ,  $-39.1$  and  $-81.0$  mV; 40 mM  $\text{Ba}^{2+}$ ,  $-35.5$  and  $-62.0$  mV. Data are indicated as mean  $\pm$  SE (A and B,  $n = 7$  from 2 frogs; C,  $n = 5-6$  from 2-4 frogs).

ence in  $V_{1/2, \text{inact}}$  with or without  $\beta 3$  was 41.9 mV with 5 mM  $\text{Ca}^{2+}$  and 38.1 mV with 5 mM  $\text{Ba}^{2+}$ . In contrast, 40 mM  $\text{Ba}^{2+}$  obscured the  $\beta 3$  effect by reducing the  $G_{\text{max}}$  ratio to 1.6 and shifting  $V_{1/2, \text{inact}}$  to  $-62.0$  mV, which is  $\sim 20$  mV more positive than for 5 mM  $\text{Ba}^{2+}$  (Fig. 9) and the difference in  $V_{1/2, \text{inact}}$  with or without  $\beta 3$  was more than 10 mV smaller than for the others. Therefore, the  $\beta 3$  subunit induced a negative shift in “closed-state” inactivation with 5 mM  $\text{Ba}^{2+}$  and was substantially unchanged with 5 mM  $\text{Ca}^{2+}$ , whereas a higher concentration of  $\text{Ba}^{2+}$  masked the  $\beta 3$  effect. The slight positive shift of  $V_{1/2, \text{act}}$  and  $V_{1/2, \text{inact}}$  with 5 mM  $\text{Ca}^{2+}$  compared with 5 mM  $\text{Ba}^{2+}$  may be due to the binding of  $\text{Ca}^{2+}$  to surface charged groups and/or a “specific regulatory site” (Zamponi and Snutch, 1996) in addition to

charge screening, whereas  $Ba^{2+}$  only possesses a charge screening ability (see Hille, 2001).

## DISCUSSION

In this study, we investigated the effect of  $\beta 3$  subunit on macroscopic current amplitude of N-, R-, and L-type calcium channels expressed in *Xenopus* oocytes. The  $\beta 3$  subunit, like other  $\beta$  subunits, has been shown to increase current amplitude by 2–30-fold in P/Q- (De Waard and Campbell, 1995; Sandoz et al., 2001), N- (Lin et al., 1997; Stephens et al., 2000; Canti et al., 2001), R- (Jones et al., 1998), and L-type (Castellano et al., 1993; Yamaguchi et al., 1998; Gerster et al., 1999; Xu and Lipscombe, 2001) calcium channels. Similarly, we found that  $Ba^{2+}$  currents through L-type channels were markedly enhanced by  $\beta 3$ . In contrast, high  $\beta 3$  levels were found to significantly suppress N- and R-type channel currents at HPs of  $-60$  and  $-80$  mV (see Table I). This effect was most prominent using recording protocols referring to physiological conditions.

### *The Effect of $\beta 3$ under More “Physiological” Conditions*

Since N- and R-type calcium channels are predominantly expressed in central and peripheral neurons (for reviews, see Wu and Saggau, 1997; Waterman, 2000) where the resting membrane potential varies from  $-55$  to  $-80$  mV (e.g., Adams and Harper, 1995; Shimizu et al., 1996; Fujimura et al., 1997; Hyllienmark and Brismar, 1999), we chose a HP of  $-60$  or  $-80$  mV to investigate the physiological characteristics of these calcium channels in the presence and absence of  $\beta 3$ . At these HPs, inhibitory effects of  $\beta 3$  were prominent, whereas at a HP of  $-120$  mV only the enhancement of the macroscopic current was observed. HPs more negative than  $-90$  mV have commonly been used to remove steady-state inactivation and to investigate the effects of auxiliary subunits on VDCC properties, where  $\beta 3$  enhancement of N- and R-type channel currents has been reported (Jones et al., 1998; Stephens et al., 2000; Canti et al., 2001). Thus, the  $\beta 3$  inhibitory effect may have been overlooked due to the use of hyperpolarized HPs.

The extracellular divalent cation concentration used as a charged carrier was found to also dramatically influence the inhibitory effect of  $\beta 3$ . The physiological extracellular  $Ca^{2+}$  concentration is  $\sim 2$  mM; however, to resolve the VDCC currents,  $10$ – $40$  mM  $Ba^{2+}$  is commonly used in the extracellular recording solution. Replacing  $5$  mM  $Ba^{2+}$  with  $5$  mM  $Ca^{2+}$  as the charge carrier, it was evident that the species of divalent cation ( $Ca^{2+}$  or  $Ba^{2+}$ ) was not so important for either  $V_{1/2, inact}$  in the presence of  $12.5$  ng  $\beta 3$  or the degree of  $\beta 3$ -induced negative shifts of inactivation, as the changes in these values by the replacement were  $< 5$  mV. However, the divalent cation concentration had a critical influence on the  $\beta 3$ -induced current inhibition as  $V_{1/2, inact}$

TABLE I  
Summary of Effects of  $\beta 3$  on  $G_{max}$  and  $V_{1/2, inact}$  of N-, R-, and L-type Calcium Channels

	Change in $G_{max}$				Shift in $V_{1/2, inact}$ (compared with control)
	HP = $-80$ mV		HP = $-120$ mV		
	Low $\beta 3$	High $\beta 3$	Low $\beta 3$	High $\beta 3$	
					mV
N-type ( $Ca_v2.2$ )	+	--	++	++	$-40$
R-type ( $Ca_v2.3$ )	+	-	+	++	$-20$
L-type ( $Ca_v1.2$ )	++	++	++	++	$+5$

+ or ++: 20–80% or  $> 80\%$  enhancement, respectively, compared with control (without  $\beta 3$ ). – or --: 10–50% or  $> 50\%$  inhibition, respectively, compared with control (without  $\beta 3$ ).

of  $-85$  mV with  $5$  mM  $Ba^{2+}$  was shifted to  $-62$  mV in the presence of  $40$  mM  $Ba^{2+}$ , resulting in obscuring the effect of  $\beta 3$ . Given that lowering the extracellular divalent cation concentration generally shifts steady-state voltage-dependent properties in a negative direction (Hille, 2001), it is expected that a physiological concentration of  $\sim 2$  mM  $Ca^{2+}$  will exhibit an even greater negative  $V_{1/2, inact}$  and more pronounced inhibition by  $\beta 3$ . Similarly, a significant influence of low divalent cation concentrations ( $2$ – $5$  mM) on L-type ( $Ca_v1.3$ ) calcium channels has been observed to produce a unique, hyperpolarized activation threshold (Xu and Lipscombe, 2001).

Under physiological condition, the mRNA or protein expression of  $\alpha_1$ ,  $\beta$ , and  $\alpha_2\delta$  subunits changes during neural development (Jones et al., 1997; Vance et al., 1998) and the expression of those subunits appears to be individually controlled (Vance et al., 1998). Therefore, it is important to characterize any concentration dependence of auxiliary subunit-induced modulation of VDCC properties. Usually, however, a fixed combination of  $\alpha_1$  and  $\beta$  subunit cRNA or cDNA is injected in a concentration ratio from 1:0.3 to 1:1. In agreement with previous reports in which only current enhancement was observed, when we examined a concentration ratio of 1:0.5 for the combination of  $Ca_v2.2\alpha_1$  and  $\beta 3$  subunits at a HP of  $-80$  mV,  $\beta 3$  increased N-type calcium channel current amplitude by 1.7- or 2.6-fold compared with  $Ca_v2.2\alpha_1$  alone in the presence or absence of  $\alpha_2\delta$ , respectively. Under similar experimental conditions, an  $\sim 3$ -fold increase in current amplitude by  $\beta 3$  was observed when  $Ca_v2.2\alpha_1$  and  $\beta 3$  were coexpressed at a ratio of  $\sim 1:0.5$ ; however, higher concentrations of  $\beta 3$  were not examined (Lin et al., 1997). In a previous study, the concentration dependence of  $\beta$ -induced modulation of N-type calcium channel properties revealed two components of inactivation (Canti et al., 2001). However, current suppression induced by higher concentrations of  $\beta 3$  was not observed at a HP

of  $-100$  mV (Canti et al., 2001). It is difficult to confirm that expression levels of  $\beta 3$  subunit in their and present studies are physiological. However, when the concentrations of  $\text{Ca}_v2.2\alpha_1$  and  $\beta 3$  were decreased while maintaining a cRNA concentration ratio of  $\alpha_1$ :  $\beta 3$  of 1:5, a similar inhibitory effect of  $\beta 3$  was observed (unpublished data). This suggests that a high concentration of  $\beta 3$  is not necessary to observe this phenomenon, but a balance between  $\alpha_1$  and  $\beta 3$  subunits is more important. It is intriguing that a significant involvement of the  $\beta 3$  subunit in N-type calcium channel currents in dorsal root ganglia neurons was demonstrated using  $\beta 3$ -deficient mice and voltage-dependent inactivation of calcium channel currents observed at a HP of  $-50$  mV in wild-type mice was largely diminished in the  $\beta 3$ -deficient mice (Murakami et al., 2002). Our results are consistent with this observation and thereby suggest a role of  $\beta 3$  inhibitory effect under physiological and pathophysiological conditions.

Together, by using experimental conditions (HP, divalent cation concentration, various subunit concentration) more closely approximating normal physiological conditions, we observe a profound effect of  $\beta 3$  to inhibit N- and R-type calcium channel currents.

#### *Mechanism of $\beta 3$ -induced Current Inhibition*

At a HP of  $-120$  mV,  $\beta 3$  simply enhanced N- and R-type calcium channel currents even at higher concentrations, where the current enhancement for R-type channels was much less pronounced than for N-type channels. A similar, less pronounced enhancing effect of a  $\beta$  subunit ( $\beta 2a$ ) on R-type channels has been reported previously using oocytes (Olcese et al., 1996). The  $\beta 3$ -induced potentiation of N- and R-type channel currents is likely to be caused by enhanced channel trafficking to the plasma membrane and an increased channel open probability, which have been observed for L- and R-type channels (Jones et al., 1998; Yamaguchi et al., 1998; Gao et al., 1999; Gerster et al., 1999).

On the other hand, the mechanism of  $\beta 3$ -induced current inhibition observed at  $-80$  mV appears to be due mainly to voltage-dependent channel inactivation and therefore it is unlikely that  $\beta 3$  blocks channel trafficking as current inhibition was almost undetectable at  $-120$  mV. In the absence of the  $\alpha_2\delta$  subunit, however, higher concentrations of  $\beta 3$  also reduced N-type calcium channel currents at  $-120$  mV. Although the cause of this inhibition is not clear, it cannot be attributed to a toxic effect of excess amounts of  $\beta 3$  cRNA, since an inhibitory effect was not observed for N-, R-, and L-type channel currents in the presence of the  $\alpha_2\delta$  subunit. Steady-state inactivation of N-type channels revealed two components in the inactivation curves in the presence of  $\beta 3$ , namely HVI with the  $V_{1/2, \text{inact}}$  of approximately  $-45$  mV and LVI with a more hyperpolarized

$V_{1/2, \text{inact}}$  of approximately  $-85$  mV with 3-min HPs. Similarly, the  $V_{1/2, \text{inact}}$  values for HVI and LVI of R-type channels were approximately  $-65$  and  $-90$  mV, respectively. Thus, it was determined that the effect of  $\beta 3$  on inactivation is to transfer the channel state/composition from exhibiting HVI to LVI. The hyperpolarized  $V_{1/2, \text{inact}}$  of LVI provides a plausible explanation for the voltage-dependent current suppression by  $\beta 3$  at a HP of  $-60$  or  $-80$  mV. Prolonged HPs of 30 min induced a negative shift of inactivation curves of N-type channels with the  $V_{1/2, \text{inact}}$  of  $-54.4$  and  $-93.5$  mV for HVI and LVI, respectively, suggesting more pronounced current inhibition with a high concentration of  $\beta 3$  at a physiological range of resting membrane potential ( $-55$  to  $-80$  mV). In this study,  $\beta 3$  subunit exhibited clear biphasic, bell-shaped effects on both peak current amplitude of I-V curves and  $G_{\text{max}}$  of N-type channels at the HP of  $-80$  mV (see Table I). The concentration dependence of  $\beta 3$ -induced increase in  $G_{\text{max}}$  was found to be  $\sim 2$ -fold more sensitive to the  $\beta 3$  concentration than increase in %LVI. A similar but more pronounced ( $\sim 7$ -fold) difference in concentration dependence of increase in  $G_{\text{max}}$  and %LVI has been demonstrated previously (Canti et al., 2001). The biphasic effect of  $\beta 3$  on  $G_{\text{max}}$  at the HP of  $-80$  mV and the difference in concentration dependence strongly support two proposed models for interactions of  $\alpha_1$  and  $\beta$  subunits. The two site-model proposes that in addition to the primary "high" affinity AID that is involved in  $\beta$ -induced channel trafficking (Pragnell et al., 1994; De Waard et al., 1995), other "low" affinity interaction sites exist for  $\beta$  subunits at the COOH and  $\text{NH}_2$  terminus of R- and P/Q-type calcium channel  $\alpha_1$  ( $\text{Ca}_v2.3$  and  $2.1\alpha_1$ ) subunits (Qin et al., 1997; Tareilus et al., 1997; Walker et al., 1998, 1999). The alternate single-site model proposes that there is only one  $\beta$  subunit binding site on the  $\alpha_1$  subunit, namely AID. In this model, the affinity of AID to a  $\beta$  subunit changes from "high" to "low" after  $\alpha_1$  subunit incorporation into the plasma membrane. This results in the dissociation of the  $\beta$  subunit from the  $\alpha_1$  subunit and gives a chance of reassociation of  $\beta$  at low affinity. Fitting our data to these two models, it is assumed that  $\beta 3$  subunits at low concentrations bind to high affinity AID of  $\text{Ca}_v2.2$  or  $2.3\alpha_1$ , thereby enhancing channel expression and macroscopic currents. At higher concentrations,  $\beta 3$  subunits interact with a second low-affinity site of the  $\alpha_1$  subunits or alternatively, reassociate with AID, then promote the transfer from HVI to LVI and inhibit N- or R-type channel currents.

Together, we speculate that low concentrations of  $\beta 3$  promote the expression of channels that produce HVI and high concentrations of  $\beta 3$  transfer channel state/composition to LVI without affecting expression levels. When channels are expressed in the absence or presence of a low concentration of  $\beta$  subunits, the partici-



pation of endogenous  $\beta 3$  ( $\beta 3_{\text{xo}}$ ) in the channel composition or properties should be considered. However, based on the results obtained with exogenously applied  $\beta 3_{\text{xo}}$ , we conclude rat  $\beta 3$ -induced shift of inactivation curves from HVI to LVI was independent on the presence of  $\beta 3_{\text{xo}}$ .

In this study, we showed that the steady-state inactivation of N- and R-type calcium channels occurred in the “closed-state” and revealed extremely slow kinetics with at least two exponential components. It is surprising that the properties of inactivation were observed not only for channels coexpressed with a high concentration of  $\beta 3$  but also for channels without  $\beta 3$ . Thus, although the subunit stoichiometry of N-type channels expressed in oocytes is unclear, higher concentrations of  $\beta 3$  simply cause a negative shift of the inactivation keeping its slow and “closed-state” inactivation properties. Given that VDCC inactivation has been intensively studied in the “open-state”, the physiological role and mechanism of VDCC “closed-state” inactivation are poorly understood. The “open-state” inactivation has been classified into three types,  $\text{Ca}^{2+}$ -dependent and fast and slow voltage-dependent inactivation (for review see Hering et al., 2000). Time constants for the onset of fast and slow voltage-dependent inactivation of non-L-type (P/Q-, N-, and R-type) calcium channels range from 40 ms to 1 s (includes fast and slow components; e.g., Stephens et al., 2000; Stotz et al., 2000) and from 30 to 70 s (Sokolov et al., 2000), respectively. In this study, the time constants for fast and slow components of the N-type channel “closed-state” inactivation were  $\sim 15$  s and  $\sim 10$  min, respectively. To distinguish this process from the slow inactivation reported by Sokolov et al. (2000), we propose the term “ultra-slow” inactivation, analogous to “ultra-slow” inactivation of sodium channels (compare Todt et al., 1999).

Similar slow closed-state inactivation has been reported for native and recombinant N-type channels. In bullfrog sympathetic neurons, which predominantly express N-type calcium channels, channel inactivation was developed at HPs of  $-40$ ,  $-50$ , and  $-60$  mV from a HP of  $-80$  mV over a time range of  $\sim 10$  min with 2 mM  $\text{Ba}^{2+}$  as the charge carrier (Jones and Marks, 1989). Another slowly developed inactivation was observed using 5 mM  $\text{Ba}^{2+}$  for N-type channels ( $\text{Cav}2.2\alpha_1/\beta 3/\alpha_2\delta = 1:0.75:1$ ) expressed in *Xenopus* oocytes (Degtiar et al., 2000). In this condition, the slow inactivation was negligible when cells were held at  $-80$  mV, but became apparent at  $-70$  and  $-60$  mV over 3-min recordings. The amount of channel inactivation at  $-60$  mV after 3 min is comparable with our results obtained from steady-state inactivation with 3-min HPs when channels were expressed with 2.5 ng  $\beta 3$  ( $\text{Cav}2.2\alpha_1/\beta 3/\alpha_2\delta = 1:1:1$ ). Interestingly, syntaxin 1A promoted this slow inactivation,

but did not show a clear effect on fast inactivation (Degtiar et al., 2000).

Patil et al. (1998) proposed a “preferential closed-state inactivation” model to account for pronounced channel inactivation during a train of action potential-like waveforms compared with a single square pulse for N-, P/Q-, and R-type calcium channels. N- and R-type but not L-type channels coexpressed with  $\beta 3$  subunits exhibit the preferential closed-state inactivation (Patil et al., 1998) and  $\beta 3$ -induced current suppression (this study). Furthermore, the absence of the preferential closed-state inactivation for N-type channels coexpressed with  $\beta 2a$  subunits (Patil et al., 1998) is consistent with the lack of an inhibitory effect of  $\beta 2a$  on N-type channel currents (unpublished data). The inactivation process of N-type calcium channels occurred over several hundred milliseconds and the half time of the recovery from the inactivation at  $-100$  mV was  $\sim 300$  ms (Patil et al., 1998). This is significantly faster than the “ultra-slow” process observed here. It remains to be determined if these two “closed-state” inactivation processes have a common underlying mechanism.

#### *Possible Physiological and Pathophysiological Roles of $\beta 3$ -induced Current Inhibition*

It is interesting to consider what physiological role the  $\beta 3$  subunit-induced suppression of N- and R-type calcium channel currents may play. N- and R-type channels are expressed predominantly in presynaptic nerve terminals of central and peripheral neurons and play a critical role in neurotransmitter release (for review see Waterman, 2000; Fisher and Bourque, 2001). Given that the  $\beta 3$  subunit causes a biphasic effect on N- and R-type channel current amplitude, it appears that one role of  $\beta 3$  is enhancement of the current amplitude to promote transmitter release at synapses. However, high levels of  $\beta 3$  relative to  $\alpha_1$  inactivate these calcium channels, thereby providing a negative feedback on the current amplitude. Interestingly, syntaxin A, which triggers vesicle fusion in nerve terminals, inactivates N- and R-type channels (Degtiar et al., 2000). It is also possible that  $\beta 3$  more actively plays a role as a negative regulator for N- and R-type channels as the expression of  $\alpha_1$  and  $\beta$  subunits has been shown to be individually regulated during brain ontogeny (Jones et al., 1997; Vance et al., 1998).

The neuronal expression levels of VDCC subunits can change dramatically in diseases such as diabetes (Iwashima et al., 2001), temporal lobe epilepsy (Lie et al., 1999; Djamshidian et al., 2002) and neuropathic pain (Kim et al., 2001; Luo et al., 2001), indicating a potential pathophysiological role of the  $\beta$ -dependent current modulation. Given that the  $\beta 3$  subunit-induced current suppression is voltage dependent, the change in the resting membrane potential during hypoxia-

induced nerve injury (Fujiwara et al., 1987; Shimizu et al., 1996; Hyllienmark and Brismar, 1999) may produce different outcomes depending on the levels of  $\beta 3$  in particular neurons.

In conclusion, our results demonstrate a novel role of calcium channel  $\beta 3$  subunits as a negative regulator of N- and R-type calcium channels approaching normal physiological conditions. We show that N- and R-type calcium channels display “ultra-slow” and “closed-state” voltage-dependent inactivation, and that  $\beta 3$  causes a significant hyperpolarizing shift of the voltage-dependent inactivation.

We are grateful to Ms. Jan C. Harries for technical assistance.

This work was supported by grants from the National Health and Medical Research Council of Australia and Australian Research Council. T. Yasuda is a recipient of a UQIPRS scholarship.

Olaf S. Andersen served as editor.

Submitted: 28 October 2003

Accepted: 13 February 2004

#### REFERENCES

- Adams, D.J., and A.A. Harper. 1995. Electrophysiological properties of autonomic ganglion neurons. *In* The Autonomic Nervous System. Vol. 6. E.M. McLachlan, editor. Harwood Academic Publishers, Reading UK. 153–212.
- Bangalore, R., G. Mehrke, K. Gingrich, F. Hofmann, and R.S. Kass. 1996. Influence of L-type Ca channel  $\alpha_2/\delta$ -subunit on ionic and gating current in transiently transfected HEK 293 cells. *Am. J. Physiol. Heart Circ. Physiol.* 270:H1521–H1528.
- Berridge, M.J. 1997. Elementary and global aspects of calcium signalling. *J. Physiol.* 499:291–306.
- Bezprozvanny, I., R.H. Scheller, and R.W. Tsien. 1995. Functional impact of syntaxin on gating of N-type and Q-type calcium channels. *Nature.* 378:623–626.
- Bichet, D., V. Cornet, S. Geib, E. Carlier, S. Volsen, T. Hoshi, Y. Mori, and M. De Waard. 2000. The I-II loop of the  $\text{Ca}^{2+}$  channel  $\alpha_1$  subunit contains an endoplasmic reticulum retention signal antagonized by the  $\beta$  subunit. *Neuron.* 25:177–190.
- Brust, P.F., S. Simerson, A.F. McCue, C.R. Deal, S. Schoonmaker, M.E. Williams, G. Velicelebi, E.C. Johnson, M.M. Harpold, and S.B. Ellis. 1993. Human neuronal voltage-dependent calcium channels: studies on subunit structure and role in channel assembly. *Neuropharmacology.* 32:1089–1102.
- Canti, C., Y. Bogdanov, and A.C. Dolphin. 2000. Interaction between G proteins and accessory subunits in the regulation of 1B calcium channels in *Xenopus* oocytes. *J. Physiol.* 527:419–432.
- Canti, C., A. Davies, N.S. Berrow, A.J. Butcher, K.M. Page, and A.C. Dolphin. 2001. Evidence for two concentration-dependent processes for  $\beta$ -subunit effects on  $\alpha 1B$  calcium channels. *Biophys. J.* 81:1439–1451.
- Castellano, A., X. Wei, L. Birnbaumer, and E. Perez-Reyes. 1993. Cloning and expression of a third calcium channel  $\beta$  subunit. *J. Biol. Chem.* 268:3450–3455.
- Catterall, W.A. 2000. Structure and regulation of voltage-gated  $\text{Ca}^{2+}$  channels. *Annu. Rev. Cell Dev. Biol.* 16:521–555.
- Chien, A.J., X. Zhao, R.E. Shirokov, T.S. Puri, C.F. Chang, D. Sun, E. Rios, and M.M. Hosey. 1995. Roles of a membrane-localized  $\beta$  subunit in the formation and targeting of functional L-type  $\text{Ca}^{2+}$  channels. *J. Biol. Chem.* 270:30036–30044.
- Coppola, T., R. Waldmann, M. Borsotto, C. Heurteaux, G. Romey, M.G. Mattei, and M. Lazdunski. 1994. Molecular cloning of a murine N-type calcium channel  $\alpha 1$  subunit. Evidence for isoforms, brain distribution, and chromosomal localization. *FEBS Lett.* 338: 1–5.
- De Waard, M., and K.P. Campbell. 1995. Subunit regulation of the neuronal  $\alpha_{1A}$   $\text{Ca}^{2+}$  channel expressed in *Xenopus* oocytes. *J. Physiol.* 485:619–634.
- De Waard, M., D.R. Witcher, M. Pragnell, H. Liu, and K.P. Campbell. 1995. Properties of the  $\alpha_1$ - $\beta$  anchoring site in voltage-dependent  $\text{Ca}^{2+}$  channels. *J. Biol. Chem.* 270:12056–12064.
- Degtiar, V.E., R.H. Scheller, and R.W. Tsien. 2000. Syntaxin modulation of slow inactivation of N-type calcium channels. *J. Neurosci.* 20:4355–4367.
- Djamshidian, A., R. Grassl, M. Seltenhammer, T. Czech, C. Baumgartner, M. Schmidbauer, W. Ulrich, and F. Zimprich. 2002. Altered expression of voltage-dependent calcium channel  $\alpha_1$  subunits in temporal lobe epilepsy with Ammon’s horn sclerosis. *Neuroscience.* 111:57–69.
- Dubel, S.J., T.V. Starr, J. Hell, M.K. Ahljianian, J.J. Enyeart, W.A. Catterall, and T.P. Snutch. 1992. Molecular cloning of the  $\alpha 1$  subunit of an  $\omega$ -conotoxin-sensitive calcium channel. *Proc. Natl. Acad. Sci. USA.* 89:5058–5062.
- Ertel, E.A., K.P. Campbell, M.M. Harpold, F. Hofmann, Y. Mori, E. Perez-Reyes, A. Schwartz, T.P. Snutch, T. Tanabe, L. Birnbaumer, et al. 2000. Nomenclature of voltage-gated calcium channels. *Neuron.* 25:533–535.
- Feng, Z.P., M.I. Arnot, C.J. Doering, and G.W. Zamponi. 2001. Calcium channel  $\beta$  subunits differentially regulate the inhibition of N-type channels by individual  $G\beta$  isoforms. *J. Biol. Chem.* 276: 45051–45058.
- Fisher, T.E., and C.W. Bourque. 2001. The function of  $\text{Ca}^{2+}$  channel subtypes in exocytotic secretion: new perspectives from synaptic and non-synaptic release. *Prog. Biophys. Mol. Biol.* 77:269–303.
- Fujimura, N., E. Tanaka, S. Yamamoto, M. Shigemori, and H. Higashi. 1997. Contribution of ATP-sensitive potassium channels to hypoxic hyperpolarization in rat hippocampal CA1 neurons in vitro. *J. Neurophysiol.* 77:378–385.
- Fujiwara, N., H. Higashi, K. Shimoji, and M. Yoshimura. 1987. Effects of hypoxia on rat hippocampal neurones *in vitro*. *J. Physiol.* 384:131–151.
- Gao, B., Y. Sekido, A. Maximov, M. Saad, E. Forgacs, F. Latif, M.H. Wei, M. Lerman, J.H. Lee, E. Perez-Reyes, et al. 2000. Functional properties of a new voltage-dependent calcium channel  $\alpha_2\delta$  auxiliary subunit gene (*CACNA2D2*). *J. Biol. Chem.* 275:12237–12242.
- Gao, T., A.J. Chien, and M.M. Hosey. 1999. Complexes of the  $\alpha_{1C}$  and  $\beta$  subunits generate the necessary signal for membrane targeting of class C L-type calcium channels. *J. Biol. Chem.* 274:2137–2144.
- Gerster, U., B. Neuhuber, K. Groschner, J. Striessnig, and B.E. Flucher. 1999. Current modulation and membrane targeting of the calcium channel  $\alpha_{1C}$  subunit are independent functions of the  $\beta$  subunit. *J. Physiol.* 517:353–368.
- Gurnett, C.A., R. Felix, and K.P. Campbell. 1997. Extracellular interaction of the voltage-dependent  $\text{Ca}^{2+}$  channel  $\alpha_2\delta$  and  $\alpha_1$  subunits. *J. Biol. Chem.* 272:18508–18512.
- Hering, S., S. Berjukow, S. Sokolov, R. Marksteiner, R.G. Weiss, R. Kraus, and E.N. Timin. 2000. Molecular determinants of inactivation in voltage-gated  $\text{Ca}^{2+}$  channels. *J. Physiol.* 528:237–249.
- Hille, B. 2001. Ion Channels of Excitable Membranes. Third edition. Sinauer Associates, Inc., Sunderland, MA. 646 pp.
- Hohaus, A., M. Poteser, C. Romanin, N. Klugbauer, F. Hofmann, I. Morano, H. Haase, and K. Groschner. 2000. Modulation of the smooth-muscle L-type  $\text{Ca}^{2+}$  channel  $\alpha 1$  subunit ( $\alpha 1C-b$ ) by the  $\beta 2a$  subunit: a peptide which inhibits binding of  $\beta$  to the I-II

- linker of  $\alpha 1$  induces functional uncoupling. *Biochem. J.* 348:657–665.
- Hyllienmark, L., and T. Brismar. 1999. Effect of hypoxia on membrane potential and resting conductance in rat hippocampal neurons. *Neuroscience*. 91:511–517.
- Isom, L.L., K.S. De Jongh, and W.A. Catterall. 1994. Auxiliary subunits of voltage-gated ion channels. *Neuron*. 12:1183–1194.
- Iwashima, Y., A. Abiko, F. Ushikubi, A. Hata, K. Kaku, H. Sano, and M. Eto. 2001. Downregulation of the voltage-dependent calcium channel (VDCC)  $\beta$ -subunit mRNAs in pancreatic islets of type 2 diabetic rats. *Biochem. Biophys. Res. Commun.* 280:923–932.
- Jones, S.W., and T.N. Marks. 1989. Calcium currents in bull frog sympathetic neurons. II. Inactivation. *J. Gen. Physiol.* 94:169–182.
- Jones, L.P., S.K. Wei, and D.T. Yue. 1998. Mechanism of auxiliary subunit modulation of neuronal  $\alpha_{1E}$  calcium channels. *J. Gen. Physiol.* 112:125–143.
- Jones, O.T., G.M. Bernstein, E.J. Jones, D.G. Jugloff, M. Law, W. Wong, and L.R. Mills. 1997. N-type calcium channels in the developing rat hippocampus: subunit, complex, and regional expression. *J. Neurosci.* 17:6152–6164.
- Kaneko, S., C.B. Cooper, N. Nishioka, H. Yamasaki, A. Suzuki, S.E. Jarvis, A. Akaike, M. Satoh, and G.W. Zamponi. 2002. Identification and characterization of novel human  $Ca_v2.2$  ( $\alpha_{1B}$ ) calcium channel variants lacking the synaptic protein interaction site. *J. Neurosci.* 22:82–92.
- Kim, D.S., C.H. Yoon, S.J. Lee, S.Y. Park, H.J. Yoo, and H.J. Cho. 2001. Changes in voltage-gated calcium channel  $\alpha_1$  gene expression in rat dorsal root ganglia following peripheral nerve injury. *Brain Res. Mol. Brain Res.* 96:151–156.
- Klugbauer, N., L. Lacinova, E. Marais, M. Hobom, and F. Hofmann. 1999. Molecular diversity of the calcium channel  $\alpha_2\delta$  subunit. *J. Neurosci.* 19:684–691.
- Lie, A.A., I. Blumcke, S.G. Volsen, O.D. Wiestler, C.E. Elger, and H. Beck. 1999. Distribution of voltage-dependent calcium channel beta subunits in the hippocampus of patients with temporal lobe epilepsy. *Neuroscience*. 93:449–456.
- Lin, Z., S. Haus, J. Edgerton, and D. Lipscombe. 1997. Identification of functionally distinct isoforms of the N-type  $Ca^{2+}$  channel in rat sympathetic ganglia and brain. *Neuron*. 18:153–166.
- Luo, Z.D., S.R. Chaplan, E.S. Higuera, L.S. Sorkin, K.A. Stauderman, M.E. Williams, and T.L. Yaksh. 2001. Upregulation of dorsal root ganglion  $\alpha_2\delta$  calcium channel subunit and its correlation with allodynia in spinal nerve-injured rats. *J. Neurosci.* 21:1868–1875.
- Mori, Y., T. Friedrich, M.S. Kim, A. Mikami, J. Nakai, P. Ruth, E. Bosse, F. Hofmann, V. Flockerzi, T. Furuichi, et al. 1991. Primary structure and functional expression from complementary DNA of a brain calcium channel. *Nature*. 350:398–402.
- Murakami, M., B. Fleischmann, C. De Felipe, M. Freichel, C. Trost, A. Ludwig, U. Wissenbach, H. Schwegler, F. Hofmann, J. Hescheler, et al. 2002. Pain perception in mice lacking the  $\beta 3$  subunit of voltage-activated calcium channels. *J. Biol. Chem.* 277:40342–40351.
- Neely, A., X. Wei, R. Olcese, L. Birnbaumer, and E. Stefani. 1993. Potentiation by the  $\beta$  subunit of the ratio of the ionic current to the charge movement in the cardiac calcium channel. *Science*. 262:575–578.
- Nowicky, M.C., A.P. Fox, and R.W. Tsien. 1985. Three types of neuronal calcium channel with different calcium agonist sensitivity. *Nature*. 316:440–443.
- Olcese, R., A. Neely, N. Qin, X. Wei, L. Birnbaumer, and E. Stefani. 1996. Coupling between charge movement and pore opening in vertebrate neuronal  $\alpha_{1E}$  calcium channels. *J. Physiol.* 497:675–686.
- Patil, P.G., D.L. Brody, and D.T. Yue. 1998. Preferential closed-state inactivation of neuronal calcium channels. *Neuron*. 20:1027–1038.
- Pragnell, M., M. De Waard, Y. Mori, T. Tanabe, T.P. Snutch, and K.P. Campbell. 1994. Calcium channel  $\beta$ -subunit binds to a conserved motif in the I-II cytoplasmic linker of the  $\alpha_1$ -subunit. *Nature*. 368:67–70.
- Qin, N., R. Olcese, E. Stefani, and L. Birnbaumer. 1998. Modulation of human neuronal  $\alpha_{1E}$ -type calcium channel by  $\alpha_2\delta$ -subunit. *Am. J. Physiol. Cell Physiol.* 274:C1324–C1331.
- Qin, N., D. Platano, R. Olcese, E. Stefani, and L. Birnbaumer. 1997. Direct interaction of  $G\beta\gamma$  with a C-terminal  $G\beta\gamma$ -binding domain of the  $Ca^{2+}$  channel  $\alpha_1$  subunit is responsible for channel inhibition by G protein-coupled receptors. *Proc. Natl. Acad. Sci. USA*. 94:8866–8871.
- Sandoz, G., D. Bichet, V. Cornet, Y. Mori, R. Felix, and M. De Waard. 2001. Distinct properties and differential  $\beta$  subunit regulation of two C-terminal isoforms of the P/Q-type  $Ca^{2+}$ -channel  $\alpha_{1A}$  subunit. *Eur. J. Neurosci.* 14:987–997.
- Scott, V.E., M. De Waard, H. Liu, C.A. Gurnett, D.P. Venzke, V.A. Lennon, and K.P. Campbell. 1996.  $\beta$  subunit heterogeneity in N-type  $Ca^{2+}$  channels. *J. Biol. Chem.* 271:3207–3212.
- Shimizu, H., A. Mizuguchi, and M. Aoki. 1996. Differential responses between CA1 pyramidal cells and granule cells to ischemic insult in rat hippocampal slices. *Neurosci. Lett.* 203:195–198.
- Shistik, E., T. Ivanina, T. Puri, M. Hosey, and N. Dascal. 1995.  $Ca^{2+}$  current enhancement by  $\alpha_2/\delta$  and  $\beta$  subunits in *Xenopus* oocytes: contribution of changes in channel gating and  $\alpha 1$  protein level. *J. Physiol.* 489:55–62.
- Snutch, T.P., J.P. Leonard, M.M. Gilbert, H.A. Lester, and N. Davidson. 1990. Rat brain expresses a heterogeneous family of calcium channels. *Proc. Natl. Acad. Sci. USA*. 87:3391–3395.
- Sokolov, S., R.G. Wei, E.N. Timin, and S. Hering. 2000. Modulation of slow inactivation in class A  $Ca^{2+}$  channels by  $\beta$ -subunits. *J. Physiol.* 527:445–454.
- Stephens, G.J., K.M. Page, Y. Bogdanov, and A.C. Dolphin. 2000. The  $\alpha 1B$   $Ca^{2+}$  channel amino terminus contributes determinants for  $\beta$  subunit-mediated voltage-dependent inactivation properties. *J. Physiol.* 525:377–390.
- Stotz, S.C., J. Hamid, R.L. Spaetgens, S.E. Jarvis, and G.W. Zamponi. 2000. Fast inactivation of voltage-dependent calcium channels. A hinged-lid mechanism? *J. Biol. Chem.* 275:24575–24582.
- Tareilus, E., M. Roux, N. Qin, R. Olcese, J. Zhou, E. Stefani, and L. Birnbaumer. 1997. A *Xenopus* oocyte  $\beta$  subunit: evidence for a role in the assembly/expression of voltage-gated calcium channels that is separate from its role as a regulatory subunit. *Proc. Natl. Acad. Sci. USA*. 94:1703–1708.
- Todt, H., S.C. Dudley, Jr., J.W. Kyle, R.J. French, and H.A. Fozzard. 1999. Ultra-slow inactivation in  $\mu Na^+$  channels is produced by a structural rearrangement of the outer vestibule. *Biophys. J.* 76:1335–1345.
- Trimmer, J.S. 1998. Regulation of ion channel expression by cytoplasmic subunits. *Curr. Opin. Neurobiol.* 8:370–374.
- Vance, C.L., C.M. Begg, W.L. Lee, H. Haase, T.D. Copeland, and M.W. McEnery. 1998. Differential expression and association of calcium channel  $\alpha_{1B}$  and  $\beta$  subunits during rat brain ontogeny. *J. Biol. Chem.* 273:14495–14502.
- Wakamori, M., G. Mikala, and Y. Mori. 1999. Auxiliary subunits operate as a molecular switch in determining gating behaviour of the unitary N-type  $Ca^{2+}$  channel current in *Xenopus* oocytes. *J. Physiol.* 517:659–672.
- Wakamori, M., G. Mikala, A. Schwartz, and A. Yatani. 1993. Single-channel analysis of a cloned human heart L-type  $Ca^{2+}$  channel  $\alpha_1$  subunit and the effects of a cardiac  $\beta$  subunit. *Biochem. Biophys. Res. Commun.* 196:1170–1176.

- Walker, D., D. Bichet, K.P. Campbell, and M. De Waard. 1998. A  $\beta_4$  isoform-specific interaction site in the carboxyl-terminal region of the voltage-dependent  $\text{Ca}^{2+}$  channel  $\alpha_{1A}$  subunit. *J. Biol. Chem.* 273:2361–2367.
- Walker, D., D. Bichet, S. Geib, E. Mori, V. Cornet, T.P. Snutch, Y. Mori, and M. De Waard. 1999. A new  $\beta$  subtype-specific interaction in  $\alpha_{1A}$  subunit controls P/Q-type  $\text{Ca}^{2+}$  channel activation. *J. Biol. Chem.* 274:12383–12390.
- Walker, D., and M. De Waard. 1998. Subunit interaction sites in voltage-dependent  $\text{Ca}^{2+}$  channels: role in channel function. *Trends Neurosci.* 21:148–154.
- Waterman, S.A. 2000. Voltage-gated calcium channels in autonomic neuroeffector transmission. *Prog. Neurobiol.* 60:181–210.
- Williams, M.E., P.F. Brust, D.H. Feldman, S. Patthi, S. Simerson, A. Maroufi, A.F. McCue, G. Velicelebi, S.B. Ellis, and M.M. Harpold. 1992. Structure and functional expression of an  $\omega$ -conotoxin-sensitive human N-type calcium channel. *Science.* 257:389–395.
- Witcher, D.R., M. De Waard, H. Liu, M. Pragnell, and K.P. Campbell. 1995. Association of native  $\text{Ca}^{2+}$  channel  $\beta$  subunits with the  $\alpha_1$  subunit interaction domain. *J. Biol. Chem.* 270:18088–18093.
- Wu, L.-G., and P. Saggau. 1997. Presynaptic inhibition of elicited neurotransmitter release. *Trends Neurosci.* 20:204–212.
- Xu, W., and D. Lipscombe. 2001. Neuronal  $\text{Ca}_v1.3\alpha_1$  L-type channels activate at relatively hyperpolarized membrane potentials and are incompletely inhibited by dihydropyridines. *J. Neurosci.* 21:5944–5951.
- Yamaguchi, H., M. Hara, M. Strobeck, K. Fukasawa, A. Schwartz, and G. Varadi. 1998. Multiple modulation pathways of calcium channel activity by a  $\beta$  subunit. Direct evidence of  $\beta$  subunit participation in membrane trafficking of the  $\alpha_{1C}$  subunit. *J. Biol. Chem.* 273:19348–19356.
- Yasuda, T., R.J. Lewis, and D.J. Adams. 2002. A novel role of the  $\beta_3$  subunit in negative regulation of N-type calcium channels. *Biophys. J.* 82:575a.
- Zamponi, G.W. 2001. Determinants of G protein inhibition of presynaptic calcium channels. *Cell Biochem. Biophys.* 34:79–94.
- Zamponi, G.W., and T.P. Snutch. 1996. Evidence for a specific site for modulation of calcium channel activation by external calcium ions. *Pflugers Arch.* 431:470–472.